Radio astronomical practical course at the Stockert 25-m telescope

Version 1.0

Jürgen Kerp

July 12, 2022

Contents

CHAPTER 1

How to use this manuscript

This manuscript provides a compact overview aiming to help you preparing the tasks you need to perform during this practical course. We focus on the basic aspects of radio telescopes and the receiving systems as well as on the data acquisition and reduction. You are going to explore the interstellar medium of the Milky Way galaxy and of a nearby galaxy by a HI 21-cm line observations. Finally you study the dispersion of a pulsar's signal. For these aims you need to find your target at the sky and to calibrate your instruments.

Chapter 2 provides an overview on the Galactic interstellar medium, the HI 21-cm line at the basic components of a pulsar, the observable quantities and the gas dynamics traceable via the Doppler-shift of the 21-cm line radiation, the coherence of electromagnetic waves, the pulsar signal's dispersion etc.

Chapter 3 compiles information on the important observational quantities like fluxes and intensities as well as their units, the Rayleigh-Jeans approximation, concept of brightness temperature.

Chapter 4 introduces the technical concept of radio telescopes and their receivers. In particular the Heterodyne principle, the radiometer equation, angular resolution and aperture blocking, antenna und brightness temperature.

Chapter 5 comprises the basic commands you have to execute during the data reduction. This session allows you to calibrate your observations, determine the system temperature and to evaluate the mass of an external galaxy. These tools you are going to use during this course. Also the basic data reduction of the pulsar measurement is presented as well as a tool to calculate the visibility of a celestial source above the horizon of the Stockert observatory.

The appendix comprises the short description of this radio astronomical observing course and a copy of the paper of Kalberla et al. (1982) on the flux calibration of HI 21-cm line observations.

Note, the PDF version of the manuscript includes hyperlinks to some internet resources.

CHAPTER 2

Introduction

2.1 Telecommunication as the origin of radio astronomy

Nearly 100 years ago, astronomy at radio wavelengths was considered not to contribute significantly to the understanding of the physics of the universe. At that time only thermal radiation processes were known, well described by the Planck law. Stellar surfaces radiate dominantly at visible wavelength. At radio frequencies, their photospheric emission is orders of magnitudes fainter than at optical wavelengths, at the first glance simply negligible. Already at that period of time radio transmission technology was successfully used for telecommunication. About 1901 Guglielmo Marconi established the first transatlantic communication. He used long wavelengths (about 350m). At these wavelengths the Earth's ionosphere is used as a mirror reflecting the long wavelength signal back to the ground. Even multiple subsequent reflections between sea and ionosphere allow the transmission of information across the whole Earth. The combination of both effects – the faintness of the Sun's black body radiation and the reflection of radio waves at the ionosphere – suggests that radio waves from outer space hardly reach Earth's ground. Despite these discouraging thoughts at the 19th of September 1901 the French astronomer Charles Nordmann tried to detect the Sun at frequencies between 0.3 and 3MHz at an altitude of 3100m in the French Alps. They failed to detect the thermal emission of the Sun at radio wavelengths. Supporting the doubts against radio astronomy.

Distortions in the quality of the telecommunication connections led the Bell Laboratory Company in the 1930 to search for their origins. Karl Jansky (Fig. 2.1) was in charge to study the systematics of these distortions. Next to thunderstorms he discovered an increase of noise reccuring every 23 hours and 56 minutes. Jansky identified that this periodic increase of noise is associated with a unique celestial source. He identified the location of this radio source with the center of the Milky Way galaxy. The emission Karl Jansky discovered is of non-thermal origin. Inserting the brightness temperatures received by his antenna in the Rayleigh-Jeans approximation yields "unrealistic" high temperatures, exceeding by far the common temperature ranges of stellar photospheres. This non-thermal radio emission is caused by fast (relativistic) moving electric charges (electrons) in magnetic fields, so-called synchrotron emission. Much later, in 1944 synchrotron emission was subject to physical considerations and the emission process was identified.

Despite Jansky's major discovery, astronomers did not start efforts to explore the universe by radio waves. The amateur radio operator and professional radio engineer Grote Reber (Fig. 2.2) started the exploration the radio emission of the Milky Way Galaxy on his own expenses. Guided by the Rayleigh-Jeans approximation with $B_\nu \propto \nu^2$ he started his

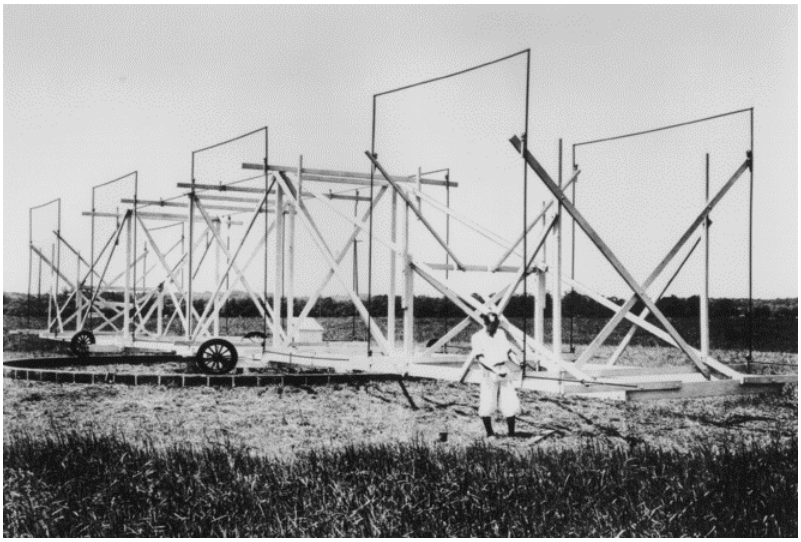

Figure 2.1: Karl Jansky in front of his 15 MHz antenna. Because Bell Telephone Company offered transatlantic telephone services, sources reducing the quality of these telephone calls were investigated systematically by Karl Jansky. The antenna is movable in the azimuth, allowing to point towards the sources of unwanted noise. Image from NRAO/AUI/NSF.

Figure 2.2: Grote Reber sitting in front of his receiving system. Image from NRAO/AUI/NSF. Reber invented radio astronomy as a research field by his systematic attempts to map the Milky Way galaxy radio continuum emission.

exploration at 3000 MHz. Reber's breakthrough however happened at 160 MHz. At these low frequencies the synchrotron emission is luminous.

After World War II radio telescope equipment were available all over the world, because radar technology was already highly developed during the war.

Until today, the photospheric radio emission of main sequence stars, except the Sun, is too faint to be detected with a state-of-the-art radio telescope. In the next decade the Square Kilometer Array(SKA) is going to provide this capability to observe main sequence stars.

2.2 The Interstellar Medium of the Milky Way Galaxy

The interstellar medium (ISM) of the Milky Way galaxy consists mainly of dust and gas.

"Dust" is commonly used as an acronym for massive agglomerations of Carbon and Silicate structures emitting at longer wavelengths as a Black Body. However, there is a huge size spectrum of the dust grains, reaching from μm to heavy molecules consisting of tens to hundreds of spinning atomic structures.

"Gas" denotes a complex composition of atomic and molecular constituents. Primarily hydrogen because of its cosmic dominant abundance due to the formation of elements during the big bang nucleo synthesis. Next in abundance is helium and carbon subplemented by some rare heavier elements, commonly named in astronomy as "metalls".

Dust and gas are exposed to the electromagnetic radiation of a manifold of different sources. Next to the billion of stars in the Milky Way Galaxy, the extra-galactic background objects heat and ionize dust and gas by their strong and high energy radiation. Due to the photoelectric effect the surfaces of the large dust grains as positively charged and adheasion attracts atoms and ions onto them, eventually forming molecules.

Dynamical processes, driven in the simplest case by the Galactic rotation, alters the size-spectrum of the dust grains and heats/cools the dust by strong volume density variations.

At the first glance, the situation appears to be hopelessly complex. A straightforward and meaningful description appears to be out of reach. But connecting our interest with the relevant linear scales on tens ot astronomical units to parsecs and accounting for the sensitivity of the performed observations allows a fair representation by local thermal equilibrium conditions. At even larger angular scales, tens of degrees or even larger, the Galactic ISM appears to be well ordered and describable by simple hydrostatic equilibrium equations.

For this observational course we need to investigate only hydrogen. Because of its abundance all metalls can be safely considered as minor ´´contamination´´. We are going to investigate the neutral phase of the atomic hydrogen by HI 21-cm line measurements. Here, we need to understand the basic technological concept to observe this line. We need to understand the local-standard-of-rest concept and the calibration of HI observations.

The ionized hydrogen will be investigated by pulsar dispersion measurements. Pulsars produce a broad band pulsed signal ranging from γ–rays to long radio waves. Because energy of that pulsed electromagnetic signal is transfered through the ionized interstellar medium, the electron component of that gas transfers high and low frequency electromagnetic radiation at different group velocities. Leading eventually to a dispersion of the signal,

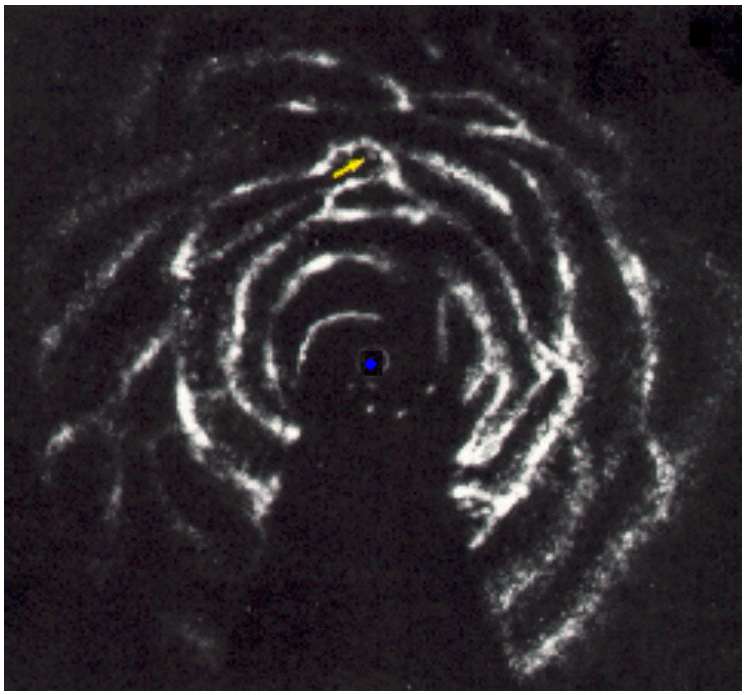

Figure 2.3: The first map of the Milky Way galaxy HI 21-cm line distribution was made in the 1950s. Note, that this is an artist representation of the observational data. At that time no electronic devices were available to extract this information from the observations. The position of the Galactic center is indicated by the blue dot, the position of the Sun by the yellow arrow. Picture from Kerr 1962

meaning different arrival times of different wavelengths of the same pulse. This is what you are going to measure and to quantify.

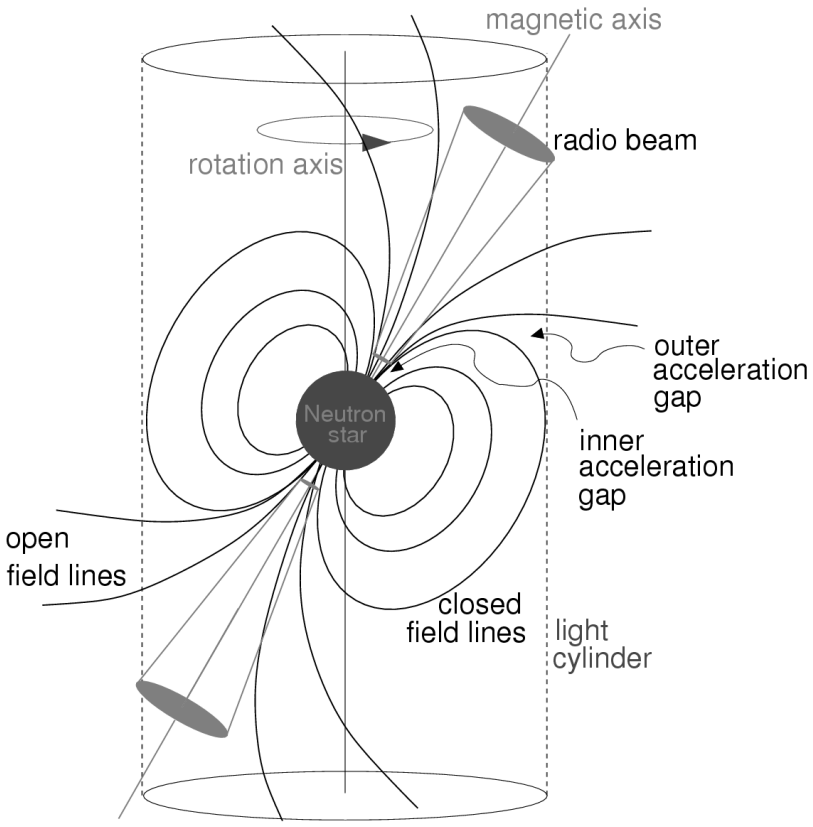

Figure 2.4: Sketch of the basic concept of a pulsar. Basically a pulsar is a neutron star. About a solar mass is compressed to a volume of a 15 km small body. The matter reaches volume densities comparable with that of an atomic nucleus. In the case that the rotational axis is tilted against the magnetic axis, a pulsating electromagnetic signal is observable. Along the magnetic axis electromagnetic radiation can escape from the neutron star's surface. Only in the case that the magnetic field axis is aligned with the observers line of sight, we will detect this pulsing signal. In all other cases we observe simply the black body radiation of a neutron star. Picture from Essentials in radio astronomy

2.3 Pulsars: dispersion of signals

Pulsars are magnetized neutron stars. During a core-collapse supernovae (i.e. Supernova Typ II) the stellar interior of a massive star forms a stellar end-point. In the case that this stellar end-point is a neutron star a mass of about 1 to 3 $M_\odot$ is concentrated within a spherical volume of about 15km diameter. Inserting some numbers on mass and volume immediately shows that the volume density is on par with an atomic nucleus. Because the angular momentum of the initial star is conserved, the compression of a tens of million kilometer star to only 15 km increases the rotation frequency by many orders of magnitude. Along with the compression of matter the magnetic forces are enhanced proportional. Pulsars show up with the strongest magnetic fields in the universe. In the case that the rotational axis has a tilt against the magnetic field, astronomers observe periodic light emission. Analog to a lighthouse the observer's telescope needs to be illuminated by the light cone focussed by the magnetic field. The period of the light flashes is a function of the rotation period of the pulsar. Typically we observe ms to s pulsars. In the case that the "lighthouse" cone fails to illuminate the radio telescope the astronomer does not observe a luminous pulsar but the faint black body radiation of a compact object.

The pulsar spectrum at radio wavelength follows roughly $\nu^{-1.7}$. It is bright at low frequencies and faint at high frequencies. With the Stockert telescope we observe the pulsars signals at 1.4 GHz, a rather low frequency. Thus, we receive strong signals. The pulsar pulse is detectable from γ-rays to longest radio waves. This broad band spectrum allows to investigate the signal creation close to the surface of the neutron star but also allows to probe the transfer of the pulsed frequency package through the galactic interstellar medium.

The Milky Way interstellar medium transfers the electromagnetic waves. It is not a vacuum, but close to. About 1 atom per cubic-centimeter is a good approximation for the volume density of the interstellar matter. Due to the illumination of the ISM by ionizing radiation i.e. by hot stellar photospheres of O and B-stars, a non-negligible fraction of that ISM is ionized. The ionization faction of the ISM is low. On average only 0.03 electrons per cubic-centimeter are observed, or 3% of the ISM is ionized on average.

The electric and magnetic components of the electromagnetic wave considered here are interacting with the free charges according to Maxell's laws. Because of the high mass of the nuclei their response to the applied force $\vec{F} = e \cdot \vec{E}$ of the electromagnetic wave is negligible in comparison to the response of the electrons. The electric field component E i.e. shakes the electron and the moved charge emits electromagnetic radiation. However its response is delayed relative to the incident wave front. The delay is caused by the environmental conditions of the moving electron. Nearby charges affect the motion via their Coulomb forces. Density, chemical composition and the number density of the free charges determine the environmental conditions of the moving charge. To handle this complex situation we quantify the delay by considering the velocity of the electromagnetic wave through the ISM like a electromagnetic wave in a dispersive medium. In such a medium the velocity of a wave package is lower than the vacuum speed of light and this

velocity is a function of frequency. We use the approach

$$v_{\mathrm{G}} = \mu \cdot \mathrm{c} \tag{2.1}$$

μ is the refractive index of the ISM and v_{G} is the group velocity of our wave. c denotes the speed of light in a perfect vacuum. The group velocity $v_{\mathrm{G}} \leq$c because the Milky Way ISM is not a vacuum. v_{G} is the velocity which describes the change of the amplitude of a wave front.

Comparing the time that a signal needs to travel a certain distance with that the same signal needs in vacuum we find a temporal delay of

$$\Delta t = \int_0^d \frac{dl}{v_{\mathrm{G}}} - \frac{d}{c} \tag{2.2}$$

Δt is the temporal offset between the wave package transferred via the ISM and the time d/c a wave package needs in a perfect vacuum. So far we do not identify a frequency dependence. Solving the Maxwell curl equations yields for the ionized portion of the ISM

$$t[\mathrm{s}] = \left(\frac{e^2}{2\pi n_e c}\right) \int_0^d n_e dl \cdot \nu^{-2}[\mathrm{MHz}] \tag{2.3}$$

Here, n_e is the electron density and ν the observing frequency in MHz. The electron density is the parameter that describes the wave propagation and is a function of frequency. Not explicitly give here but used for the derivation of the equation above is the so-called plasma frequency $\nu_p = \left(\frac{e^2 \cdot n_e}{\pi \cdot m_e}\right)^{\frac{1}{2}}$ which is under typical ISM conditions about 0.3 kHz. Below that plasma frequency a signal can not be transferred. Above that frequency the signal is transfered but with different velocities for different frequencies. The plasma frequency desribes the response of the ionized gas to the incident electromagnetic radiation.

For the ISM we use here

$$t[\mathrm{s}] \simeq 4.15 \cdot 10^3 \int_0^d n_e dl \cdot \nu^{-2}[\mathrm{MHz}] \tag{2.4}$$

The quantity

$$DM = \int_0^d n_e dl [pc \cdot cm^{-3}] \tag{2.5}$$

DM is called the **dispersion measure** and can be directly inferred from radio astronomical observations.

Pulsar's with their luminous and very well characterized radio flashes are ideal objects to study the dispersion measure of the ISM. Observing a pulsar will disclose the time delay of

the different frequencies of a single wave package. One needs to adopt only an appropriate electron volume density to estimate the distance to the pulsar.

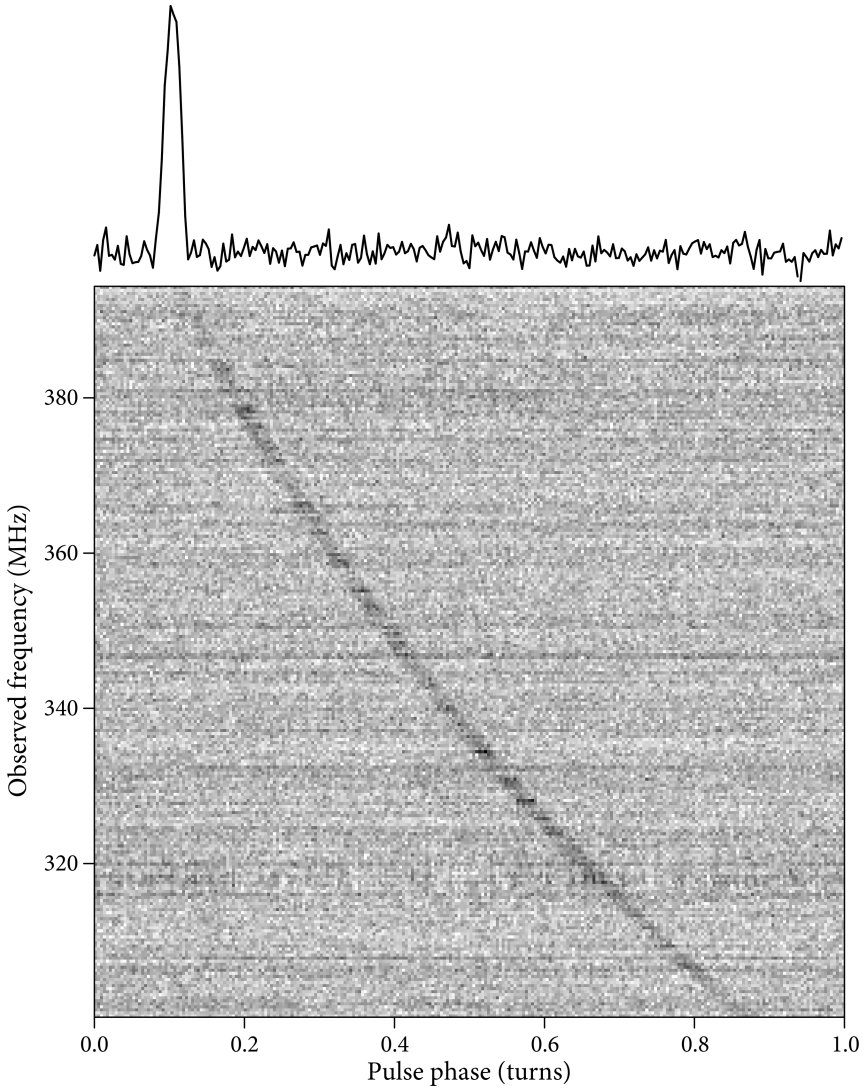

Figure 2.5: Dispersion of a pulsar wave package. The gray scale plot shows the temporal delay ν^{-2} as a function of frequency versus the pulse phase toward pulsar J1400+50. Picture from Essentials in radio astronomy

2.4 The neutral atomic hydrogen line at 21-cm wavelength

The HI 21-cm line was theoretically predicted as ideal tracer for the dynamics and mass distribution of the Milky Way galaxy by Hendrik van der Hulst. Hydrogen is the most abundant element in space because it was formed already during the big bang nucleo synthesis. Despite the fact that the largest fraction of hydrogen is nowadays contained in stars, huge amounts of neutral hydrogen are still distributed along all lines of sight through the Milky Way galaxy.

The HI 21-cm line became observationally accessible in 1951. Ewen and Purcell at Harvard, Muller and Oort in the Netherlands and Pawsey in Sydney announced the multiply confirmed detection of the HI 21-cm line in the September 1. issue of *Nature* Ewen & Purcel 1951. In the 1950s and 1960s the primary aim of 21-cm line observation was the exploration of the Milky Way disk. Because of the optical appearance of external galaxies the scientist at that time expected to verify the spiral structure of the Milky Way galaxy. The Leiden-Sydney map (Fig: 2.3) presented by Oort in 1958 confirmed this expectation.

Neutral atomic hydrogen (HI) is of special interest not only because of its outstanding abundance. Optical light from distant stars is strongly attenuated by the intervening dust, this process is called extinction. Photons having energies of a few eV do not allow to disclose the large scale structure of the Milky Way galaxy. The HI 21-cm hydrogen emission line is in contrast to them ideally suited for that task. The reason for this is that the HI line is easy to excite by inelastic collisions of atoms. This means already tiny amounts of the kinetic energy of atoms and molecules ($\sim 10^{-6}$ eV) in the interstellar space can excit the neutral hydrogen atom. Moreover the lifetime of the excited state is extreme long, it is in the order of millions of years. According to the energy-time uncertainty relation $\Delta E \times \Delta t \geq \frac{\hbar}{2}$ the natural line width (ΔE) of the 21-cm HI line is extremely narrow. For resonant absorption of a 21-cm photon the absorbing atom needs to be in a very similar physical state and additionally located exactly at the same line of sight. This is highly unlikely. Thus, HI photons travel through the Milky Way Galaxy nearly unattenuated. This transfer of electromagnetic radiation through the interstellar medium is called in astronomy as "optical thin" radiation. Meaning that each photon emitted reaches the observer without any interaction with the intervening interstellar matter. Theoretical considerations led in 1944 van der Hulst to propose that the `1s` state of neutral hydrogen offers such an optical thin transition between hydrogen's hyper-fine levels $F = 1$ and $F = 0$ state.

A photon carries a spin of 1, thus the transition from the neutral hydrogen $F = 1$ to $F = 0$ level emits a photon (see Fig. 2.6). $F = 1$ corresponds to the situation that both, the proton and electron spin are oriented in the same direction. $F = 0$ corresponds to the anti-parallel orientation of both spins. According to the tiny energy difference between both states the photon is emitted at a low frequency of 1420.405 MHz or at 21.1cm wavelength. The Einstein coefficient for this transition is $A_{10} = 2.85 \cdot 10^{-15}\,\mathrm{s}^{-1}$, thus the mean lifetime of the (excited) parallel $F = 1$ is $t = \frac{1}{A_{10}} \simeq 3.5 \cdot 10^{14}\,\mathrm{s} \simeq 11 \cdot 10^{6}$years. The $F = 1$ is populated via collision, but collision cause also radiation less de-excitation in rather high volume density environments, like molecular clouds for example. This radiation less de-excitation by collisions was the reason that it was long time not feasible to produce

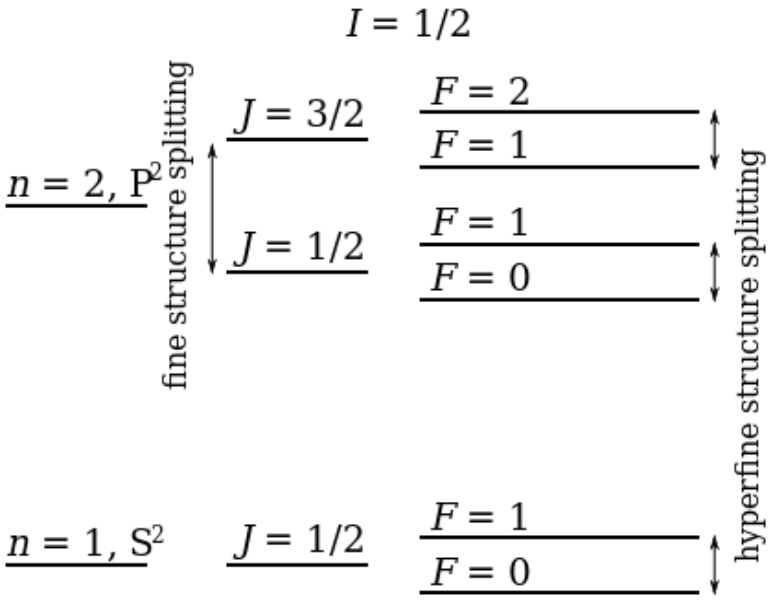

Figure 2.6: Term scheme of neutral atomic hydrogen. **Left** basic electronic levels (main quantum number) populated by optical light. **Middle** fine structure transitions cause by spin-orbit coupling causing infrared light. **Right** Hyper-fine transitions, here the spin-spin interaction causes tiny energy differences between the energy levels, in case of the ground state the difference is $5.6 \cdot 10^{-6}$eV. Image from Wikipedia.

the HI 21-cm line in a laboratory. Accordingly the HI 21-cm line belong to the class of so-called forbidden lines.

Because of $\Delta E \cdot \Delta t \geq \frac{\hbar}{2}$ the long lifetime Δt of the $F = 1$ state yields an extremely narrow ΔE line width, allowing to measure the Doppler motion precisely down to levels of $cm \cdot s^{-1}$. All in all van der Hulst identified that the 21-cm line is ideal to study the whole Milky Way galaxy. Hydrogen is the tracer for the interstellar gas in general, because of its high abundance. Its physical state is used to deduce the physical properties of the whole interstellar gas. Hydrogen is considered to be the quantitative tracer for the ISM. All other elements, the metalls, are of minor importance and the collisions with hydrogen atoms couples their thermal motion to that of hydrogen.

2.4.1 Line shape of the HI 21-cm radiation

The inelastic collisions between the atoms and molecules within the interstellar medium couples the different constituents with each other. Depending on the mass m of the particle a certain amount of kinetic energy E_{kin} leads to a mass proportional velocity $v \propto \frac{E_k}{m}$. The velocity distribution of an ensemble of particles is well described by the Maxwell distribution. This Maxwell distribution uniquely couples the velocities of the particles with a temperature T in the interstellar environment. Observing HI 21-cm line with a radio telescope and a spectrometer shows a Gaussian line shape (see Fig. 2.8). The observed line width is much broader (at full-width-at-half-maximum, FWHM) than the natural one.

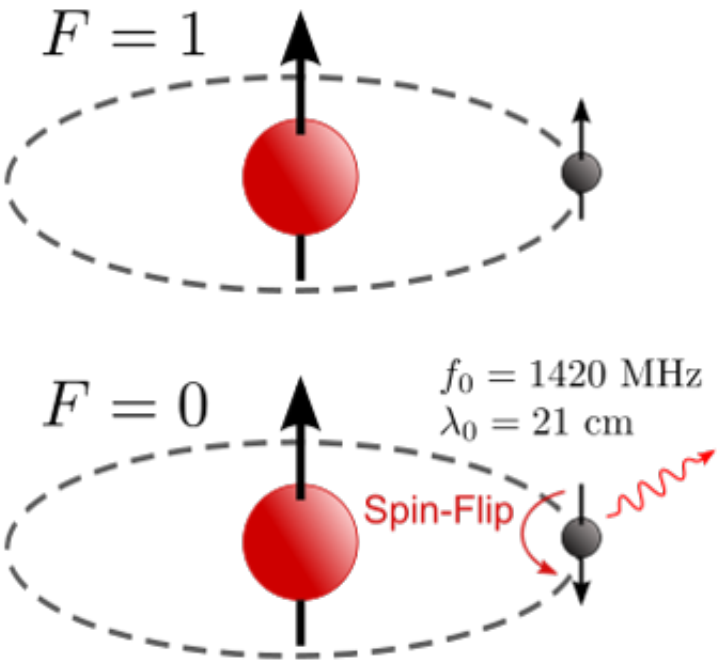

Figure 2.7: The $F = 1$ and $F = 0$ energy state illustrated by the orientation of the proton and electron spin. Image from Wikipedia.

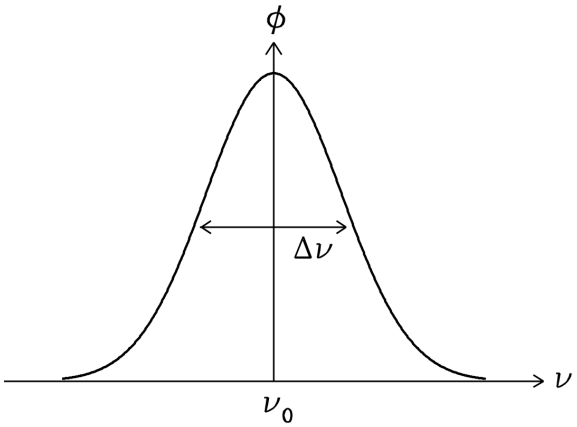

Figure 2.8: The HI 21-cm line can be described by a Gaussian. To characterize the Gaussian shape, we need only to determine next to its position (here, Doppler shift) the Full-Width-at-Half Maximum (FWHM).

Typically between 1 and 70 $\mathrm{km\,s^{-1}}$ (i.e. Kalberla & Haud (2015)). The FWHM line width is the measure for the density and turbulence of the hydrogen gas. We can not distinguish between thermal and turbulent broadening without any additional information. Thus, the observed FWHM line width is a measure for the upper limit of the kinetic gas temperature $T_{\mathrm{k}in}$

$$T_{\mathrm{k}} \leq \frac{m_{\mathrm{H}} \cdot \Delta v^2}{8 \cdot \mathrm{k}_B \cdot ln(2)}$$

The peak brightness of the Gaussian shaped HI line is proportional to the brightness temperature T_{B}. Because we observed at very long wavelength or low frequencies, this peak is a measure for the minimum gas temperature according to the *Rayleigh-Jeans* law (see Sect. 3.1).

$$B_\nu(T) \simeq \frac{2\,\nu^2\,\mathrm{k}_B\,T_{\mathrm{B}B}}{\mathrm{c}^2}$$

$T_{\mathrm{B}B}$ is the temperature of the Black Body, ν the frequency observed, c the speed of light and k_B the Boltzmann constant. B_ν is proportional to $T_{\mathrm{B}B}$ and gives a lower limit to the gas temperature.

In summary, in case that we observe an isolated (even in bulk velocity) cloud along the line of sight we can estimate a lower limit of the gas temperture by the peak of the HI line and an upper limit by the FWHM of the Gaussian shaped line profile.

2.4.2 The Local Standard of Rest

The Earth's rotates and orbits the Sun. The Sun orbits the Galactic center. Thus, we as observers are located in a moving rest frame. Since about 100 years astronomers are aware of this motion around the Galactic center. For an accurate description of that motion the local stellar environment of the Sun has been measured in velocity and a so-called local standard of rest frame has been introduced. For you as observer the telescope control system corrects automatically for all relative motions against the local standard of rest frame. You can identify this by the characters v_{LSR} denoting a velocity relative to the local-standard of rest.

Observing an external galaxy displays commonly not a gaussian shaped line. Gaussian lines of gas clouds are formed by the thermal (Maxwell velocity distribution) of the atoms. In a galaxy however, the rotation of the whole galaxy smears out the individual Gaussian line profiles of individual gas clouds. Countless individual gas clouds are superposed a single line of sight. Their different velocities adds up to the rotation curve of the galaxy. The HI clouds illuminate, in this respect, the motion of the whole galaxy. We as observers distinguish between two velocities. One is the systemic velocity. The systemic velocity is the velocity of the galaxy as an entity. It is equal to the red-shift of the galaxy and thus via the Hubble law a measure for the galaxy's distance. The other velocity is measured again via the FWHM of the galaxy HI profile but not interpreted in terms of thermal motion. A galaxy FWHM line width is a measure for the mass of the galaxy. A galaxy as an entity rotates around its center. It is stable. This means the gravitation and centrifugal forces balance each other. The larger the FWHM of the galaxy's HI line the larger the

centrifugal forces and thus the mass of the galaxy to balance them.

2.4.3 Column density and baryonic gas mass

In case of an optical thin gas cloud all photons emitted travel to the radio telescope without significant absorption or scattering. This yields that the brightness temperature and the line width are immediate measures of the total number of hydrogen atoms along the line of sight. This measure is called the *column density*

$$N_{\mathrm{HI}}[cm^{-2}] = 1.8224 \cdot 10^{18} \int \frac{T_{\mathrm{B}}}{[K]} d\left(\frac{v}{[km\,s^{-1}]}\right) \tag{2.6}$$

Here, N_{HI} denotes the *column density*, the integrated number of all neutral hydrogen atoms along the line of sight. T_B is the observed brightness temperature. The number $1.8224 \cdot 10^{18}$ is related to the Einstein coefficient A_{10}.

Evaluating the HI mass of an external galaxy is not different to the determination of the column density. We integrate across the HI line profile of the galaxy and deduce the total number of hydrogen atoms. We adopt the hypothesis that the line emission is optical thin. The structure of the equation is like for the column density but one needs to consider the $1/r^2$ law for the decrease of the intensity as a function of separation r between the source and observer.

$$\frac{M_{\mathrm{HI}}}{M_{\odot}} \simeq 2.36 \cdot 10^5 \left(\frac{r}{\mathrm{M}pc}\right)^2 \int \left(\frac{S_{\nu}}{\mathrm{J}y}\right) \cdot \left(\frac{dv}{\mathrm{km}\,s^{-1}}\right) \tag{2.7}$$

Here S_ν is the specific flux (see Sect. 4.5). What you are measure at the Stockert observatory is only the HI mass. To evaluate the total baryonic mass of a galaxy you need to take into account that the hydrogen mass M_{HI} is at most 10% of the total baryonic mass, concentrated in stars. The total mass is however a third, different thing. It includes also the dark matter and the ratio of luminous to dark matter depends strongly on the scales under consideration see Fig, 2.9. Thus, evaluating the total mass of a galaxy means to estimate the amount of dark matter relative to the measured hydrogen mass.

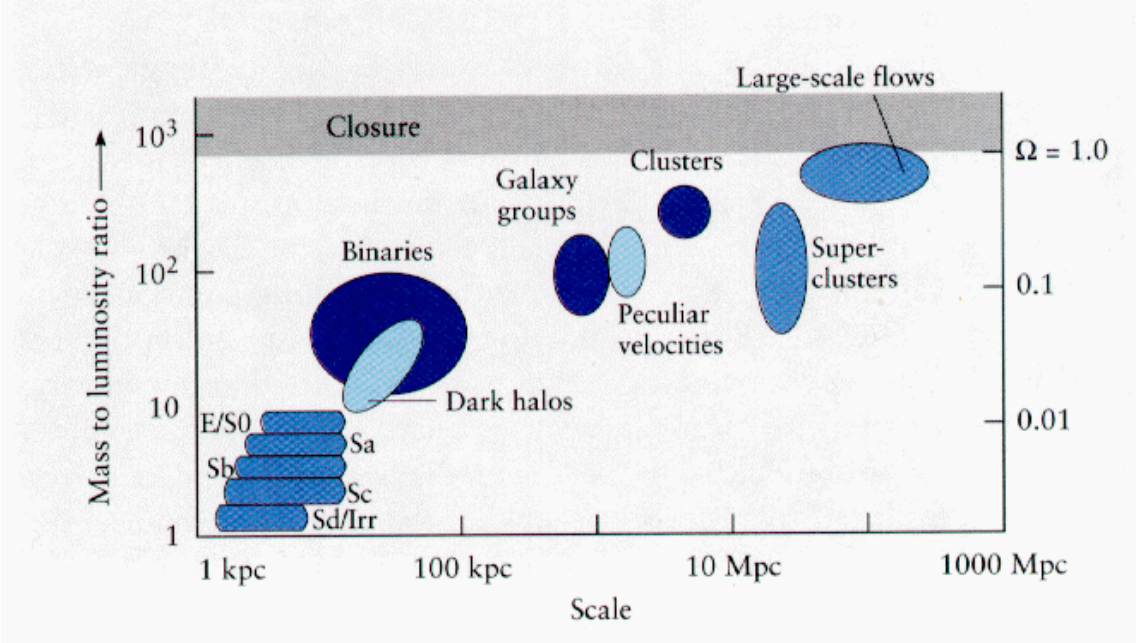

Figure 2.9: Different linear scales appear to host a different mixing of baryonic and Dark Matter. With this graph you might estimate the amount of unseen Dark Matter in your galaxy of interest. Note that we evaluate only the hydrogen mass of the ISM by our observations. This amounts only to a few percent of the baryonic mass of a galaxy. The picture has been extracted from the University of Oregon astronomy course, lecture 23

CHAPTER 3

Physical background

3.1 Thermal radio emission

The primary aim of a radio telescope is to collect and focus electromagnetic radiation. According to the Maxwell description of electromagnetic waves, they are periodically varying electric and a magnetic fields. Both are oriented perpendicular to each other. The orientation of the electric field vector allows to define a quantity, called *polarization*. In case that the electric field vector is fixed in orientation, we observe a *linearly polarized* wave. In the other case that the orientation of the electric field vector changes periodically, the electromagnetic waves is called to be *circularly polarized*. As we will see below, different radiation processes reveal different polarization properties. Electromagnetic radiation transfers energy. Commonly we use the photon representation to evaluate the amount of energy transferred by the wave $E = \mathrm{h}\nu$.

Electromagnetic waves are emitted when a charged particle is accelerated. In the radio regime we are observing wavelengths from dm to sub–mm. This wavelengths interval corresponds to frequencies in the range from MHz to THz. Quantifying the Planck constant in units of eV $\mathrm{h} = 4.135 \cdot 10^{-15}\,\mathrm{eV}\,s^{-1}$ yields $4 \cdot 10^{-9} \leq \mathrm{h}\nu[eV] \leq 4 \cdot 10^{-4}$. These are really low photon energies compared to the average kinetic energy of the moving particle in a typical gas within the Milky Way galaxy ($\mathrm{k}T \sim 8.62 \cdot 10^{-5}\,\frac{J}{K} \times 1000\,K \simeq 0.08$). We find $\mathrm{h}\nu \ll \mathrm{k}T$. Here, k denotes the Boltzmann constant with $8.617 \cdot 10^{-5}\,\mathrm{eV}\,K^{-1}$ and T the gas temperature.

Let us consider the brightness $B_\nu(T)$ according to the Planck law and $\mathrm{h}\nu \ll \mathrm{k}T$

$$B_\nu(T) = \frac{2\mathrm{h}\nu^3}{\mathrm{c}^2} \frac{1}{e^{\frac{\mathrm{h}\nu}{\mathrm{k}T}} - 1} \tag{3.1}$$

with

$$e^x = 1 + x + \frac{x^2}{2!} + \frac{x^3}{3!} + ... \tag{3.2}$$

we find for $\frac{\mathrm{h}\nu}{\mathrm{k}T} \ll 1$

$$B_\nu(T) = \frac{2\nu^2 \mathrm{k}T}{\mathrm{c}^2} \tag{3.3}$$

For thermal (black body) emission, the brightness $B_\nu(T)$ of an observed source is directly

proportional to the so-called brightness temperature T. Thus, at radio wavelengths we observe directly the physical temperature of the emitting source.

3.2 Coherence of cosmic electromagnetic radition

Almost all sources of electromagnetic radiation are located at huge distances from the observer. According to the Huygens-Fresnel principle, the spherical waves approach the Earth's observer as almost perfect plane waves. Moreover, the individual waves appear in some sense to be synchronized. This means that the strengths of the electric and magnetic fields as well as the phases of the electromagnetic waves observed at Earth are fixed. In that case we speak about *coherence*. Coherence describes the ability of electromagnetic radiation to *interfere*. Adding different waves yields a new wave, different in amplitude and phase to the incident ones, but again with a unique frequency and amplitude. This is mathematically described by the van Cittert-Zernicke theorem.

Electromagnetic waves from all distant space objects have the ability to interfere. This is of major importance for astronomical observations, because it allows to construct telescopes as interferometers. This statement is correct for the whole electromagnetic spectrum, ranging from radio telescopes to X-ray and γ-ray observatories. At Earth however, the different atmospheric layers attenuate the radiation of the cosmic objects or degrade the coherence for certain wavelength ranges of the cosmic waves, leading finally to incoherent radiation. The twinkling of the stars at visible wavelengths is due to destructive interference. Turbulence cells in the Earth's tropospheric layer have different refractive indicies due to varying densities and temperatures. This is however not any issue for dm to sub-mm wavelengths. Allowing to construct radio telescopes as interferometers at ground like the Jansky Very Large Array (JVLA), the Atacama Large Millimeter Array (ALMA) and the Square Kilometer Telescope(SKA).

3.3 Intensity, brightness and power

Staying in the photon representation of an electromagnetic wave, the amount of energy a photon is carrying is $E = \mathrm{h}\nu$. Now, what is intensity I_ν? I_ν denotes the *s*pecific intensity and is a quantitative measure for the number of photons (or amount of energy) radiated at the frequency ν. The amount of energy we are receiving from a certain portion of the sky

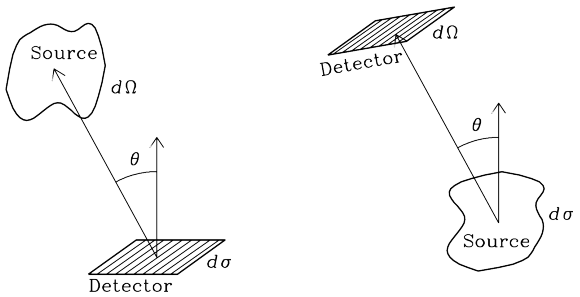

Figure 3.1: Orientation of the source and detector θ to each other is important to calculate the flux received. The extent of the source across the sky is denoted as dΩ. Picture from Essentials in radio astronomy

depends on its area $d\Omega$ across the sky, the area of the detector $d\sigma$ we are using and the orientation θ between the plane of our detector and the direction to the source of interest. Obviously, in the case that θ is zero, the source and the detector plane are oriented parallel to each other, maximizing the number of photons. Accordingly, if we integrate across a certain period of time dt we receive a certain amount of energy dE.

$$dE = I_\nu \; d\Omega \; d\sigma \; d\nu \; cos(\theta) \; dt \; [\mathrm{J}] \tag{3.4}$$

The power we are receiving from a source is simply

$$dP[Watt] = \left(\frac{dE}{dt}\right) = I_\nu \; d\Omega \; d\sigma \; d\nu \; cos(\theta) \, [m^2 \; sr \; s^{-1}] \tag{3.5}$$

reordering the equation yields

$$I_\nu = \frac{dP}{d\Omega \; d\sigma \; d\nu \; cos(\theta)} \, [W \; m^{-2} \; sr^{-1} \; s] \tag{3.6}$$

The quantity I_ν is called *specific intensity* or *spectral brightness*.

3.3.1 The solid angle

A solid angle of a calotte with the opening angle θ can be calculated via

$$d\Omega = 2\pi(1 - cos(\theta)) \tag{3.7}$$

for very low values of θ, we find

$$d\Omega = \pi \; \theta^2 \tag{3.8}$$

Returning to the spectral brightness I_ν of a source, if we integrate the spectral brightness across the angular extent of the source we find

$$S_\nu \equiv \int_{Source} I_\nu \; cos(\theta) \; d\Omega \tag{3.9}$$

This quantity S_ν is called the *flux density* of the source, because it denotes the power dP we receive in our detector per frequency interval $d\nu$ and per detector area $d\sigma$. Because the angular extent/area of the source $d\Omega$ depends on the separation D between the Earth

and the source of interest, thus

$$S_\nu \propto \frac{1}{D^2} \tag{3.10}$$

If we integrate S_ν across whole sphere with radius d encircling the source of interest we find

$$L_\nu = S_\nu \; 4\pi \; d^2 \tag{3.11}$$

the spectral luminosity of the source interest.

Integrating the *spectral luminosity* across the all frequencies we find the *bolometric luminosity* of the source

$$L \equiv \int_\nu L_\nu \; d\nu \tag{3.12}$$

CHAPTER 4

Radio telescopes

4.1 System temperature

The radio telescope receives radiation from its whole environment. The antenna's maximum sensitivity is called the main lobe. This main lobe receives about 70% of all incomming radiation. The remaining fraction is received by the *near-* and *far-side lobes*, sometimes called as *stray lobes*. While the main lobe is comparable to the main maximum of an Airy disk, the stray-lobes are equivalent to the ring like diffraction pattern encircling the maximum of the Airy disk. Without any obstacle i.e. a lens telescope, most of the incident photons are focussed in the very center of the Airy disk, while the diffraction rings comprises only a few percent of all incident photons. Because essentially all radio telescopes suffering an apperture "blocking" hence a much larger fraction of the incident radiation is collected by the side-lobes. An unblocked aperture, like the Green-Bank Telescope receives about 84% of the incident radiation by the main lobe.

Observing a celestial source means measureing the radiation from a specific position. But many additional unwanted superimposed source of radiation contaminate the emission of the source of interest. Roughly we can differentiate five sources.

- the source of interest T_{source},

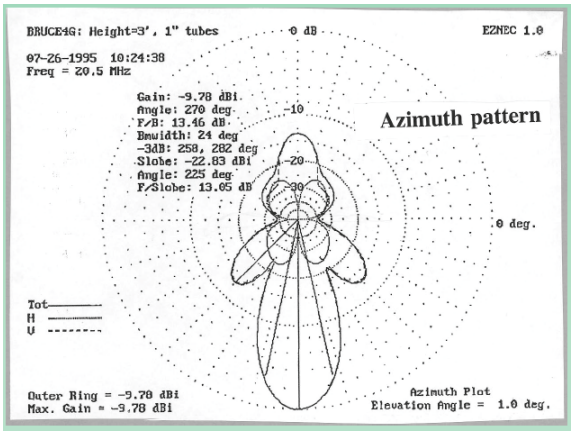

Figure 4.1: Antenna diagram or sensitivity pattern of a radio telescope. This is the antenna diagram of Karl Jansky's antenna. The main beam is straight forward to identify. Orders of magnitude less sensitive (note scaling in dB) are the stray-lobes. Even from the telescope's backside radiation is received. Essentials in radio astronomy

- the cosmic microwave background T_{CMB},
- the diffuse synchrotron radiation of the Milky Way galaxy $T_{syn}(\nu = 1420\,\mathrm{M}Hz) \simeq 0.1\,\mathrm{K}$ with $\nu^{-2.7}$,
- the warm Earth's atmosphere T_{atm}
- the spill-over T_{spill} caused by the fact that the receiver is typically optimized to view as much as possible from the primary mirror, partly it receives also radiation from beyond the edges of the primary mirror.
- the thermal noise of the receiving system $T_{receiver}$.

Because all received radiation adds up linearily, the brightness temperature received is

$$T_{sys} = T_{source} + T_{CMB} + T_{syn} + T_{atm} + T_{spill} + T_{receiver} \tag{4.1}$$

Typically your source of interest is faint. Accordingly, the emission of the source is tiny in comparison to the system temperature. To increase the signal–to–noise ratio one tries to minimize the system temperature by actively cooling the amplifier. Its thermal noise dominates the whole receiver chain, because it amplifies its noise by several thousand times. At 21-cm wavelength a typical system temperature of cooled systems is about 18 K, not actively cooled systems show up with system temperatures about a factor of three to five higher.

4.1.1 The atmospheric window

Imagine that the Earth's atmosphere is illuminated by the Black Body radiation of our close by star. We know, that the Earth's atmosphere effectively blocks (absorps) ultraviolett and X-ray emission. This radiation ionizes the outer atmospheric layers. Implying that free electrons are available. The ionisphere serves as a mirror for radio waves. We use this fact at long wavelengths for telecommunication (Sect. 2.1) but the signals of cosmic sources at the same wavelength range never reach Earth's ground. Besides to the reflection of long wavelength, there is the thermal emission of the Earth's atmosphere, which contributes significantly to the system temperature.

Atmospheric molecules absorb energy from the Sun's radiation spectrum, most important are CO_2, O_2 and in particular H_2O. Water vapor is the most important green-house molecule. Its rotational and vibrational transitions redistribute the Sun's spectral energy distribution to frequencies in the GHz to THz regime. Because molecules show up with a line spectrum, at these radio frequencies, the opacity varies appreciable close to these lines.

In Fig. 4.2 the opacity across the whole electromagnetic spectrum is presented. At the location of the radio telescope icon, the severe variation due to water vapor and O_2 are easily visible. At a few GHz to hundreds of MHz however, the atmospheric opacity is negligible. Through this huge frequency window the space is explorable from Earth's ground. At the frequency window around 1.4 GHz even water vapor does not absorb strongly. Only the continous irradiation corresponding to the physical temperature of the atmospheric layers contribute to the system temperature.

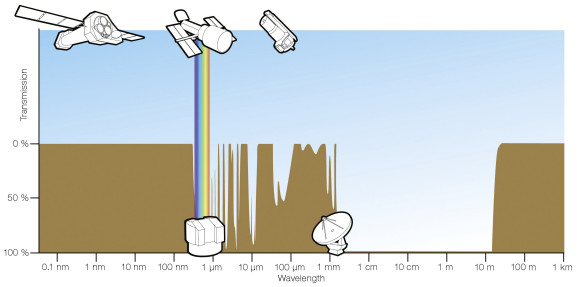

Figure 4.2: Ground-based astronomy is limited to the visible and radio atmospheric windows. In this representation it is apparent how huge the radio window is in comparison to the optical window. At very low frequencies Earth's ionosphere simply reflects the radiation back into space. Close to 1 THz the attenuation is due to the abundant molecules in Earth's troposphere. At the wavelengt of interest for the Stockert telescope, the opacity of the Earth atmosphere is negligible. Abscissa: Wavelength. Ordinate: Atmospheric transmission. Image Credit: ESA/Hubble (F. Granato).

4.1.2 Radiometer equation

The radiometer equation give us a measure for the quality of a radio astronomical observation

$$\Delta T = \frac{T_{sys}}{\sqrt{\Delta\nu \cdot \Delta t}} \tag{4.2}$$

Here, ΔT is the uncertainty in the determination of the source brightness temperature. $\Delta\nu$ is the bandwidth and Δt is the duration of the observation. The product of both is a measure for the amount of energy received $\Delta E \propto (\mathrm{h})\Delta\nu \cdot \Delta t$. The longer the integration Δt the higher the number of received photons. This holds also true in case of an increasing bandwidth $\Delta\nu$ we just receive a higher number of photons. A faint source obviously demands a long integration time Δt. T_{sys} is, as described above (Sect. 4.1), the superposition of different independent radiation sources.

4.2 Radiometer

A radiometer is the receiving unit of a radio telescope. It consists of six main parts. The first part is the receiving dipole. For wavelengths longer than 0.3m a simple dipole is used. For shorter wavelengths a *f*eed is used. This feed is optimized to convert the space waves, with a minimum of losses, into an electric current in the receiving dipole placed at a certain position within the feed.

Because the radio astronomical sources are very faint, we need a high amplification of the incident signal. A simple amplifier is a transistor. The basic idea of a transistor is, that a strong current between the *source* and the *drain* of the transistor is modulated by the weak signal linked to the *gate* of the transistor. Thus tiny modulations in the voltages caused by the received faint signal are amplified by orders of magnitude 10^3 to 10^6 in current between the drain and the gate.

Next, we insert a bandpass. The bandpass selects a certain frequency portion of the whole electromagnetic spectrum.

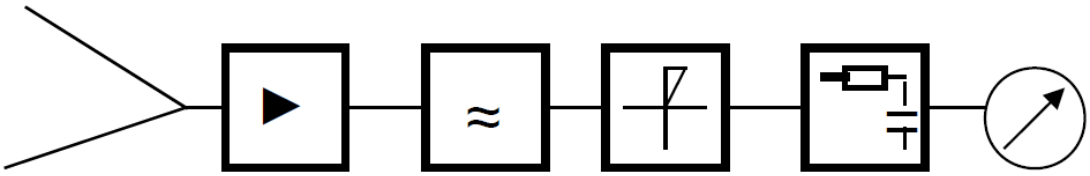

Figure 4.3: Sketch of the principal construction of a radiometer. Depending on the wavelengths of interest, the arrangement of the elements bandpass and first amplifier might change depending on construction at very high frequencies. At high frequencies a second amplification is necessary. The radiation from space enters from the left. The feed transforms the space wave. First element behind the feed is an amplifier. This amplifier has a high gain, about 10^3 to 10^6. A bandpass selects the wavelength range of interest. A diode is used to square the signal, transforming amplitude variations into intensity variations. An integrator collects the amount of energy. Finally we read-out the amount of energy with our backend.

Simply adding the changes in voltage would average out the positive and negative modulations the electromagnetic wave recorded at our receiving dipole. To evaluate the amount of energy we receive from the astronomical object, we square the signal from the amplifier U_{HF} (HF for high frequency), after passing our detector we measure a voltage U_{det} (det for after passing the detector) with $U_{\mathrm{det}} \propto {U_{\mathrm{HF}}}^2$. As detector we can simply use a diode. A diode has a strong non-linear current-voltage characteristics. At the aim-point of the diode we find the square characteristics.

Now adding up all voltage modulations U_{det} after the detector we have the signal we are searching for. As integrator we can use a simple RC circuit integrator. After the integration Δt (see Sect. 4.1.2) we read-out the integrated power.

4.2.1 The spectrometer

Using a spectrometer it is feasible to determine accurately the Doppler velocity of the 21-cm line emission. Because the HI line is extremely narrow, the frequency resolution (or velocity resolution) is in practice limited to the frequency resolution of the spectrometer. Electronic spectrometers use the Fast-Fourier Transformation (FFT). FFT spectrometers use certain correlation schemes, basically this limits the number of spectral channels to be a power of two. Typically we have 2^{14} or more spectral channels. Adopting 100MHz bandwidth at 21-cm wavelength 2^{14} spectral channels correspond finally to 6.1kHz or $1.28\mathrm{k}m \cdot s^{-1}$ in channel separation.

4.2.2 Noise of the radiometer elements

Each individual element of the radiometer produces noise. This is because our equipment is a physical structure exposed to its environment. Consider the motion of the electrons in each element. According to the Maxwell-Boltzmann distribution the physical temperature of a device is proportional to the velocity distribution of the electrons. Statistical motions of electrons produce a random signal in our receiver. The higher the physical temperature

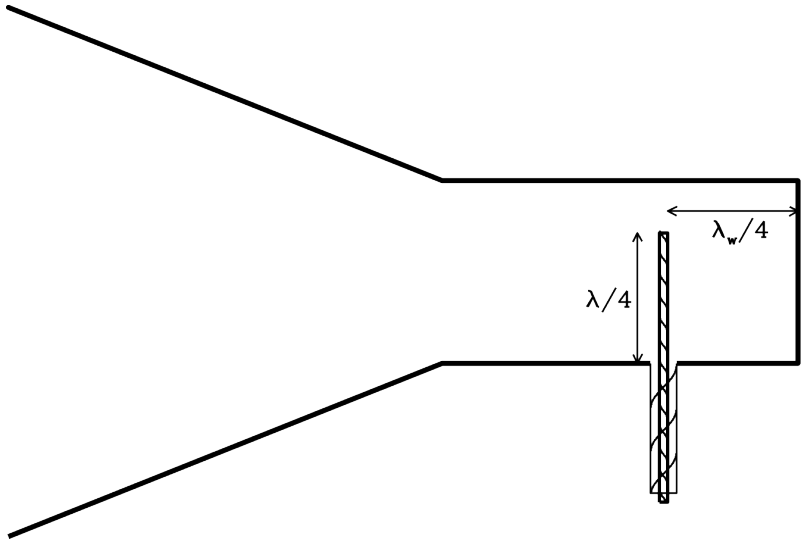

Figure 4.4: The feed converts the space wave into an electric wave. Its form has to be optimize for each radiometer. The real antenna is the dipole placed at a certain position in the feed.

of a device the higher the velocity of the electrons. Because it is a random motion its signature will be identified as noise. In the case that we lower the physical temperature of the element we lower the mean velocity of the electrons and accordingly the noise.

Of highest importance for the receiver temperature is obviously the first element. Its physical temperature determines the quality of the receiver. This first element is typically an amplifier. Its gain G_1 is about 10^3 to 10^6, thus the noise added by the physical temperature of the next element following is reduced in the averaging calculation by $T_2/G_1 \ll T_1$ (see Fig. 4.5). Consequently, the first element of a radiometer is actively cooled by liquid nitrogen or even liquid hydrogen.

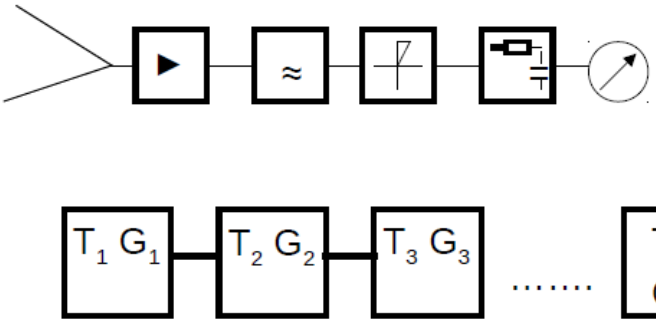

$$T = T_1 + \frac{T_2}{G_1} + \frac{T_2}{G_1 * G_2} + \ldots + \frac{T_N}{G_1 * G_2 * \ldots * G_{N-1}}$$

Figure 4.5: Top panel radiometer, **middle panel** each individual element of the radiometer has a certain physical temperature T_i and a gain G_i. **Bottom panel** In the case that the first element of the radiometer is the amplifier with a high gain G_1 the noise added to the whole signal chain by the subsequent elements is reduced by $1/G_1$. The average physical temperature of the radiometer depends essentially on the temperature of the first element.

4.3 Radio telescopes construction

Radio telescopes are constructed to collect electromagnetic radiation. The larger the dish size D, the higher the number of photons. The angular resolution is calculated as in optical astronomy. While in optical astronomy typically we have arc-seconds as common units in radio astronomy we use are arcmin for single dish telescopes. The ability to separate two unresolved sources is limited by the Half-Power-Beam Width (HPBW)

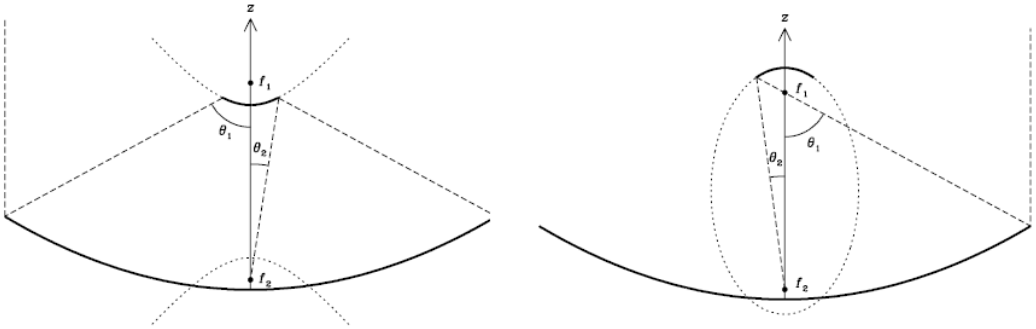

Figure 4.6: Left: optical layout of a Cassegrain telescope. **Right:** Optical design of a Gregory telescope. Image from the textbook "Essentials in radio astronomy, Chapter 3.

$$HPBW[^\circ] = 58.9 \cdot \frac{\lambda[m]}{D[m]}$$

In the case that two sources are located closer than the HPBW, we can not separate both.

Common constructions for radio telescopes are *Cassegrain* and *Gregory* telescopes. Both telescopes constructions are affected by the blocking of the aperture because of a secondary mirror. The advantage of the Cassegrain over the Gregory construction is the shorter, more compact design, minimizing the moved mass of the telescope. The major advantage of the Gregory construction is however, that an additional focus is available, the *prime focus* of the primary mirror. Receivers can accordingly installed in two foci, the primary and the secondary focus. For Cassegrain constructions only the secondary focus is accessible. Because for a Gregory system the focal length of the primary mirror f_1 is much shorter than that of the Cassegrain optics, the field of view of a primary focus receiver is large. Thus, the fast optics (large $\frac{f_1}{D}$, all collected photons are concentrated in a compact focal plane) allows high-speed recording of large portions of the sky by using multi-beam receivers (arrays).

4.3.1 Aperture blocking

As for most telescope constructions, the aperture of a radio telescopes is blocked. Blocking denotes the fact that an obstacle lowers the number of the incident photon severely. This leads to a lower sensitivity and to a degradation of the angular resolution. But beneficially, this obstacle allows to construct a rigid and compact telescope.

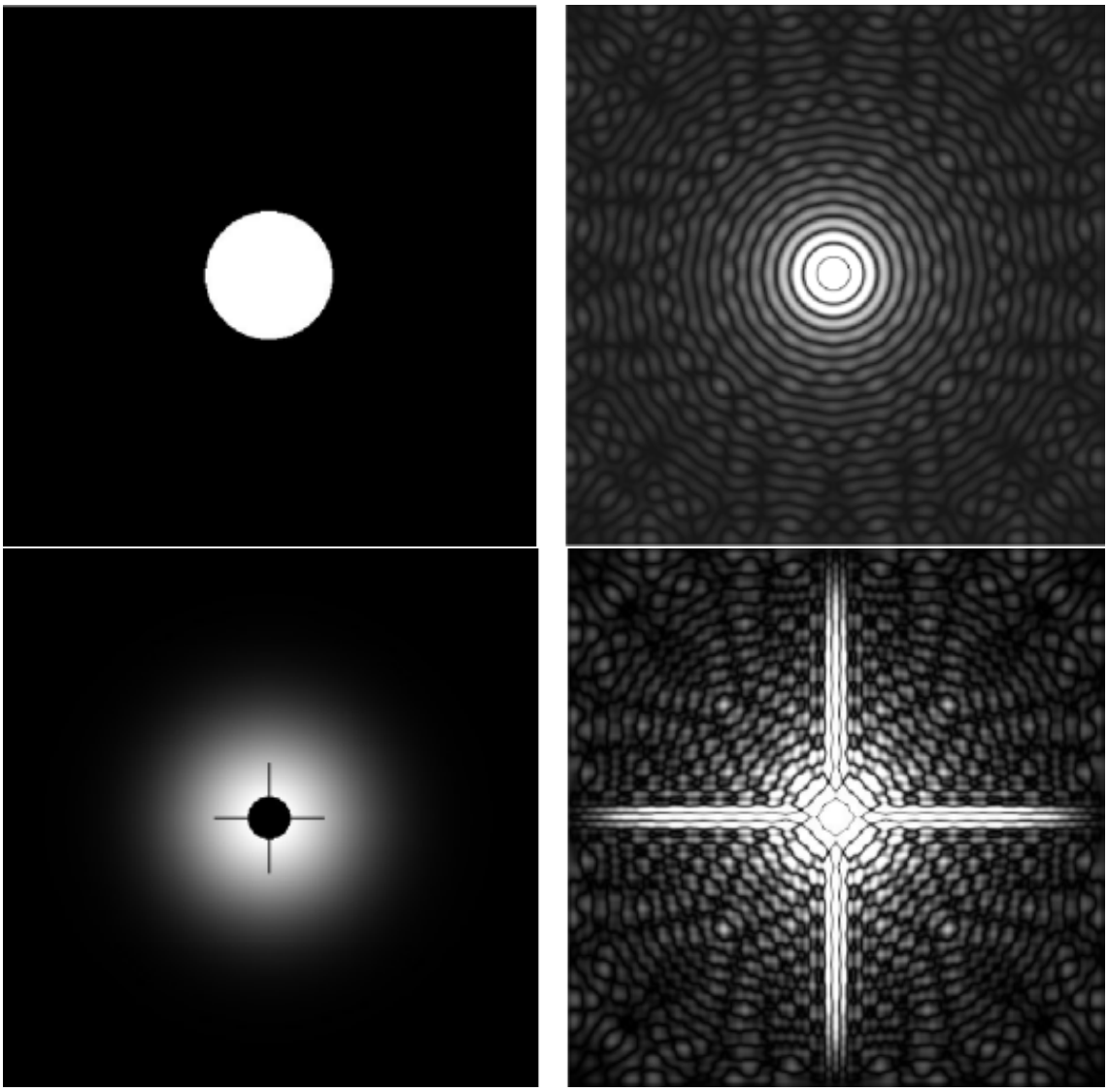

Figure 4.7: **Top left:** Ideal unblocked aperture with maximum transmission out to the rims of the telescope. **Top right:** Power distribution of the unblocked aperture. This is the well known Airy disk pattern realized in practice by a refracting telescope. **Bottom left:** Blocked aperture of a radio telescope. Because one aims to minimize the system temperature (see Sect. 4.1) one needs to minimize the *spill over* of the receiver. This is realized by a Gaussian taper here. **Bottom right:** Power distribution of that blocked aperture. The angular resolution is severely degraded (reduced) by the secondary mirror. The larger the secondary, the worse the angular resolution. The support legs cause the cross-like structure.

4.4 Antenna diagram

Above, we use a two dimensional representation of the sensitivity pattern of a radio telescope. But a radio telescope is a three dimension object. Also the sensitivity pattern of a radio telescope is 3-D. The sensitivity pattern is called the *antenna diagram*. It denotes a projection of the 3-D structure i.e. onto the azimuth. It is a common practice to use a logarithmic scaling. According to that scaling 0dB corresponds to the maximum sensitivity the main beam. The side lobe are a few tens of Decibel scale (dB) below that. At $-3\,\mathrm{dB}$ half of the maximum of the main beam sensitivity is reached, we call this the $-3\,\mathrm{dB}$ level. By construction, the side lobes can be minimized by minimizing the blockage. In contrast to optical telescopes, radio telescopes receive also radiation from the back side. Thus a strong artificial radiation sources located at the back side of the telescope, might severely degrade the observations because of their significant contribution to the total signal received. Signals of that kind, unrelated to the source of interest, are denoted as Radio Frequency Interferences (RFI).

4.4.1 Surface accuracy

Surfaces of radio telescopes appear visually to be very different. Sub-mm telescopes show partly a surface quality comparable to optical telescopes while dm radio telescopes consists of wires only. It depends on the wavelength to be observed that determines the quality of the surface. In practice we are aiming to shape the primary mirror as ideal parabola. Deviations from that shape degrade the antenna diagram. Deviation might by systematic deformations of the whole telescope constructions, leading to a spatial shift of the focus. Also the roughness of the surface degrades the imaging capabilities. Take into consideration the coherence of the incident radio waves. Thus a rough surface with distortions in the order of $\frac{\lambda}{2}$ or $\frac{\lambda}{4}$ will cause severe destructive interference and some fraction of the signal will vanish. So, we need to minimize the deviations σ with respect to the wavelength of interest λ. As a statistical measure of the quality of a mirror surface in case of a random distribution of σ as deviation from the ideal shape, statistically it is feasible to approximate these deviations by a Gaussian distribution we find the quantity η which is a measure for the smoothness of a surface. The larger σ the smaller λ the rougher the surface described quantitatively by η.

$$\eta = e^{-\left(\frac{4\pi\sigma}{\lambda}\right)^2} \tag{4.3}$$

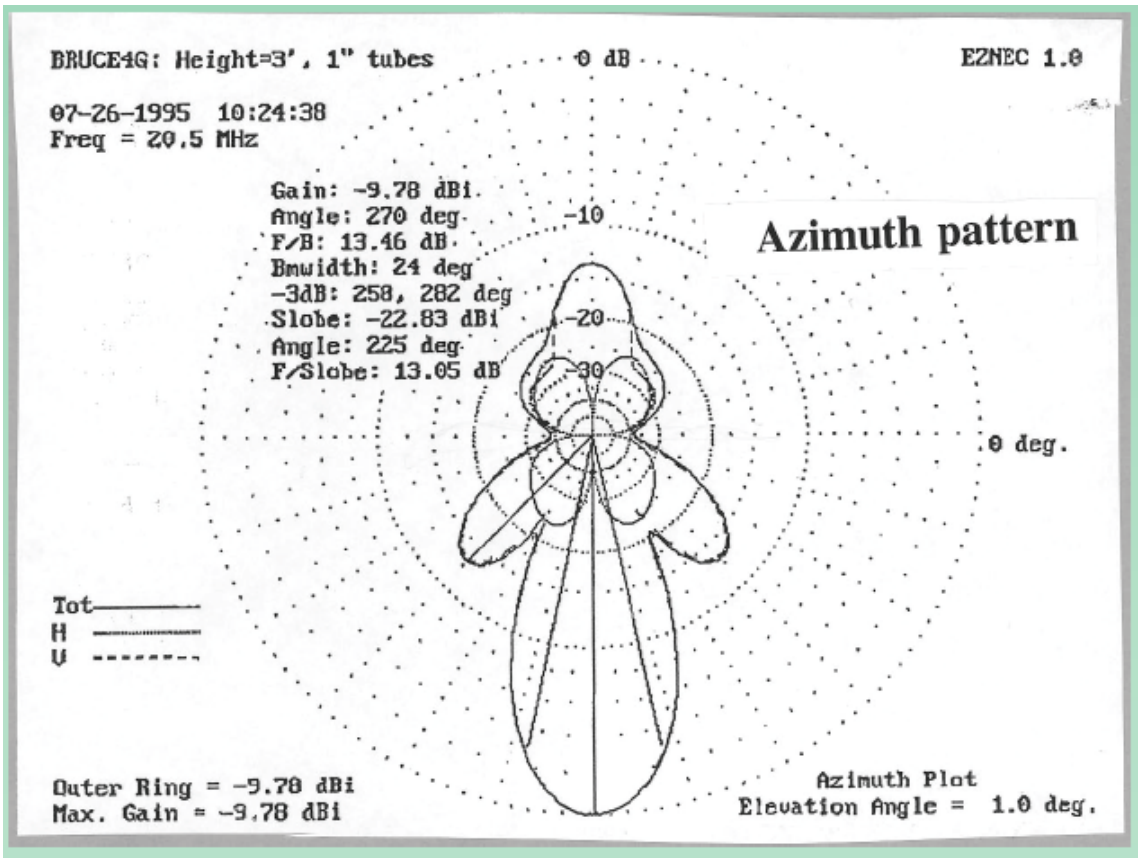

Figure 4.8: Antenna diagram (sensitivity pattern) of Karl Jansky's telescope. Shown is a projection of the 3-D antenna diagram onto the azimuth. Obviously a complex structure is displayed. Next to the main beam, side-lobes can be identified. Note that a radio telescope receives also radiation from the back side. Thus, strong artificial irradiation into these side lobes can severely degrade the quality of the observation. The sensitivity pattern is scale in dB, denoting the sensitivity contrast between main and side lobes. Typically one aims to minimize the side lobes to the -30dB level.

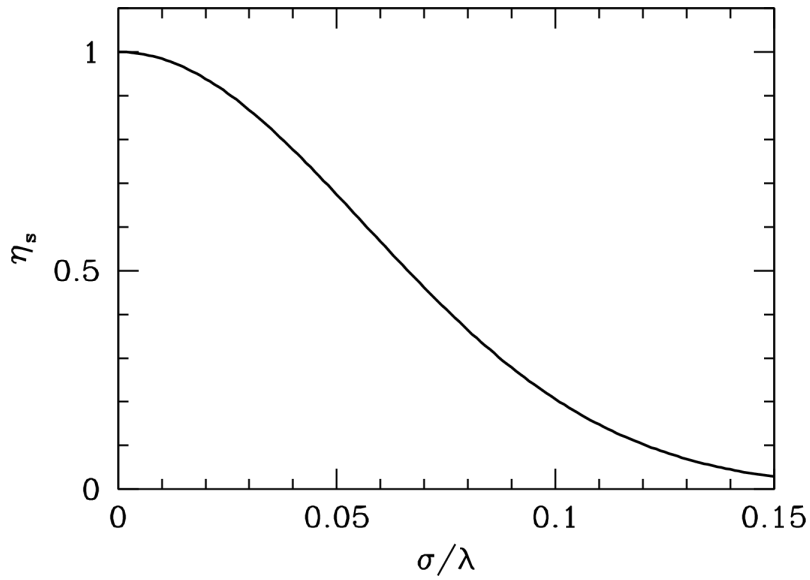

Figure 4.9: Displayed is the smoothness of the surface as a function of the ratio of the surface random variation σ and the wavelength λ. The longer the wavelength the larger the acceptable surface variations. The picture has been extracted from the textbook "Essentials in radio astronomy" chapter 3 Figure 17.

4.5 Antenna vs. brightness temperature

By deriving the Rayleigh-Jeans approximation we identified, that the received flux is proportional to the physical temperature of the emitting object (see Sect. 3.1). We call this value the *brightness temperature* T_B. But is T_B what we really measure with the radio telescope? To answer this question we need to consider the telescope beam. Typically at 21-cm wavelengths the beam has a diameter of a few tens of arcmin. Most of the radio astronomical source are far away, leading to angular extents of much less than that value. In consequence only a narrow portion of the whole beam is illuminated by the source of interest. The remaining fraction of the beam receives unrelated emission. Thus, we do not measure T_B directly but an *antenna temperature* T_A. This antenna temperature is not unique for a source of interest, it depends on the size of the telescope. Different radio telescopes will come up with different antenna temperatures.

$$\frac{T_\mathrm{A}}{T_\mathrm{B}} = \frac{\Omega_{source}}{\Omega_{\mathrm{MainBeam}}} \tag{4.4}$$

Here Ω_{source} is the angular extent of the source and $\Omega_{\mathrm{MainBeam}}$ is the angular extent of the telescope main beam. As we know from the antenna diagram, a radio telescopes receives radiation via the main beam but also via the stray lobes. A measure for the ratio between the radiation received via the main beam and the stray lobes is given by the main beam efficiency ζ

$$\zeta = \frac{\Omega_{\mathrm{mainbeam}}}{\Omega_A} \tag{4.5}$$

Here, Ω_A is the area of the antenna diagram which we can subdivide in $\Omega_{\mathrm{MainBeam}}+\Omega_{stray}$. For the calibration of a radio telescope it is necessary to observe a source with a well known flux at the frequency range of interest. For large telescopes one uses typically active galactic nuclei located at cosmological distances. Their strong synchrotron radiation allows to measure their flux accurately within a short integration time. Because these sources are also un-resolved by the telescope's beam, one use these sources also for the *pointing* of the telescope. Their coordinates at the sky are well known, thus one can compare the telescope's coordinate system relative to the true sky positions, allowing to identify errors due to the mechanical construction of the telescope.

For HI 21-cm line measurements several positions across the Milky Way Galaxy have been identified that allow to measure T_B directly. These standard calibration regions are defined by Kalberla, Mebold & Reif are sufficiently large, so that their brightness temperature distribution allows to measure T_B independently from the telescope size accurately. Moreover, the positions in radial velocity of the HI 21-cm line emission maxima allow to control the frequency calibration of the used instrumental setup. The integral across the whole line is the measure for the total flux received from that calibration region and thus our measure of interest for the calibration.

4.6 Conversion Kelvin in Jansky

The antenna temperature we measure depends essentially on the used telescope and its construction. Our aim however is to convert this to a physical quantity, independent of any detail of the used instrument. Here we use an instrumental dependent quantity called *aperture efficiency*

$$A_{\text{eff}} = \frac{P_{\text{received}}}{S_{\text{source}}} \tag{4.6}$$

P_{received} is the power we received from a source with the specific flux S_{source}.

$$A_{\text{eff}} = \frac{2 \cdot \text{k} \cdot T[\text{K}]}{S_{\text{source}}[\text{Jy}]} \tag{4.7}$$

By using the Rayleigh-Jeans approximation here. This yields

$$\frac{T[\text{K}]}{S_{\text{source}}[\text{Jy}]} = \frac{A_{\text{eff}}}{2 \cdot \text{k}} \tag{4.8}$$

This is a conversion of Kelvin in Jansky, or from brightness temperatures in mks units. Now let insert some numbers characteristic for the Stockert telescope.

$$\frac{T[\text{K}]}{S_{\text{source}}[\text{Jy}]} = \frac{\pi \cdot (12.5 \cdot 0.7\text{m})^2}{2 \cdot 1.38 \cdot 10^{-23} \left[\frac{J}{K}\right]} \cdot 10^{-26} \left[\frac{J}{m^2}\right] \tag{4.9}$$

This yields

$$\frac{T[\text{K}]}{S_{\text{source}}[\text{Jy}]} = 0.09 \tag{4.10}$$

Thus, a 1 Jy source produces a brightness temperature of about 0.1 K in our receiver.

4.7 Calibration of an HI observation and system temperature

The calibration of our Stockert HI observation as well as the determination of the system temperature is going to be performed by observing a standard position from the Kalberla et al. (1982, attached to this manuscript). For these aims please select either S7, S8 or B8. You have to make sure that the source is above the horizon during your observing session.

All these calibration sources are all located within the plane of the Milky Way galaxy. This means, the velocity profiles are rather broad. Numerous individual HI clouds are superposed on a single line of sight. Their different radial velocities sum up to the HI 21-cm line profile observed.

For these standard regions Kalberla et al. (1982) tabulated basic properties like peak brightness and the integral across the HI profile. You need to account for the baseline

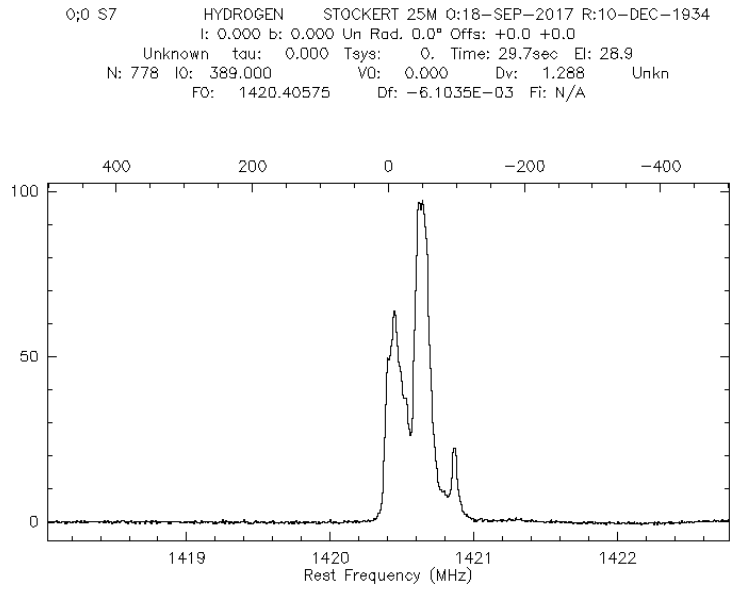

Figure 4.10: HI 21-cm line spectrum of the calibration source S7 as observed with the Stockert telescope. The HI profile displayed here is already corrected for the baseline contribution. The line profile displays the superposed emission of many different gas clouds along the line of sight, because S7 is a region located within the plane of the Milky Way galaxy.

of your observation, see next Section for a detailed description how to remove it. After removal of the baseline (see step 13 to 15 of Sect.5.1) you can evaluate the peak brightness temperature and the line integral. Note that Kalberla et al (1982) used some limits in the radial velocity for the integration of the line intensity.

Practically, you need to perform the observation. Here, you have to integrate sufficiently long to minimize the statistical uncertainties. They should be less that 5%. Than you need to subtract the baseline and determine either the peak or/and the integral across the HI line profile. Compare your results with that tabulated ones in Kalberla et al. (1982). The ratio of both values is your calibration factor. All HI spectra you are observing during your observing session needs to be multiplied with the calibration fractor α. With that you evaluate $T_B = \alpha \times T_A$.

4.8 Visibility of celestial objects

Key for all astronomical observations is the visibility of a source of interest above the observer's horizon during the observing session. To determine the so-called visibility the celestial position of the source needs to be related to the local date and time at the observatory. Moreover, the geographic latitude of the observing site determines the height of a source of interest above the horizon.

The information on the geographic location of the Stockert observatory you will find i.e. in its wikipedia entry.

Commonly astronomers are using the Universial Time (UT) for scheduling purposes.

Combining the source position with date, local time and geographic position yields the

objects visibility. A tool, you might consider to use, is airmass.org to calculate the objects visibility as a function of local time. Inserting the source's name or correspondingly its right ascension and declination yields a visibility chart. On its y-axis you will find the elevation and on the X-axis the time in UT.

4.9 Observing Galaxies

Figure 4.11 shows a HI spectrum of a nearby galaxy. Its proximity can be deduced from its low radial velocity (the Hubble-Lemaitre law allows to estimate the galaxy's distance). Here, the recessional velocity is only about $v_{\mathrm{LSR}} \simeq 240\,\mathrm{km\,s^{-1}}$ suggesting a distances of about 3.5 Mpc with $\mathrm{H_0} = 75\,\mathrm{km\,s^{-1}\,Mpc^{-1}}$. The Milky Way Galaxy HI emission is, according to the Milky Way's rotation curve, distributed in velocity symmetrically around $v_{\mathrm{LSR}} \simeq 0\,\mathrm{km\,s^{-1}}$ with maxima and minima of about $\pm 100\,\mathrm{km\,s^{-1}}$. For the selection of your galaxy of interest three major parameters are of importance: recession velocity v_{r}, peak line intensity T_{B} and area below the galaxy's line profile.

Recession velocity: Using the Hubble-Lemaitre law $v_{\mathrm{r}} = \mathrm{H_0} \cdot D$ (with v_{r} as recession velocity, $\mathrm{H_0} = 75\,\mathrm{km\,s^{-1}\,Mpc^{-1}}$ as local Hubble-Lemaitre parameter and D the distance in Mpc) the higher the recessional velocity the larger the galaxy's distance. Considering the Eq. 3.10 a low recessional velocity is a necessary condition for a high flux.

Peak line intensity: After calibrating the telescope you have an estimate of the system temperature and thus the noise. The higher the peak line intensity of a galaxy of interest, the higher the signal–to–noise ratio. Thus, a high line intensity is an obvious selection criterium.

Area below the galaxy's HI line profile: The larger the area under the galaxy's line profile the larger its HI mass. Obviously, two parameter are competing with each other, the high peak line intensity and the area under the line profile. Preferential, you are interested

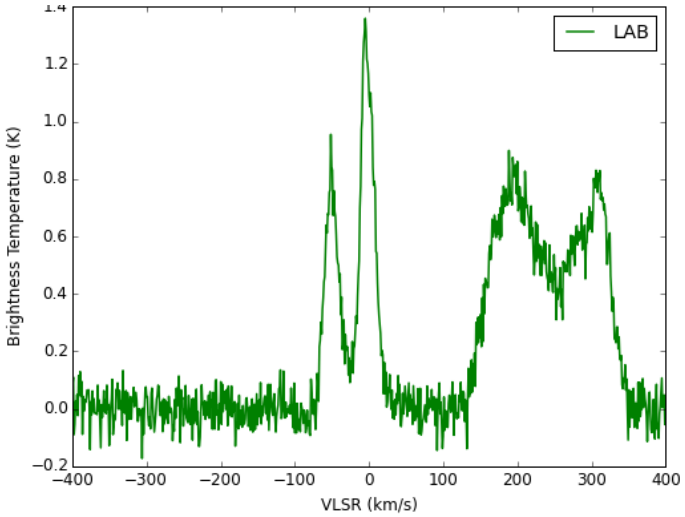

Figure 4.11: HI 21-cm line spectrum towards a spiral galaxy observed with a 25-m radio telescope at HI 21-cm. Around $v_{\mathrm{LSR}} \simeq 0\,\mathrm{km\,s^{-1}}$ the Milky Way Galaxy HI emission is visible. The HI emission of the external galaxy has its systemic velocity of $v_{\mathrm{LSR}} \simeq 240\,\mathrm{km\,s^{-1}}$.

in bright massive galaxies, those show up with a HI spectrum like in Fig. 4.11. But in the case that the width of the line profile is getting broader and broader, the total flux of the HI emission is smeared out across many spectral channels, leading to a decrease of the peak line intensity and thus to a lower signal–to–noise ratio. Thus you have to find a compromise between both quantities.

How to search for a suited galaxy? The Goddard space flight center offers a web-interface allowing to search for galaxies. Considering the points mentioned above the parameters *dec*, *radial velocity*, *h1_21_cm_mag* and *h1_21_cm_50pc_width* are of interest. They limit the height of the source above the observatory's horizon, the galaxy's distance, its HI peak line intensity and the width of the galaxy's HI line. Moreover the parameter *major axis* might be of interest. This should be much smaller than the telescope's main beam extent, otherwise your observation does not cover the whole galaxy within a single pointing. To guess the relevant parameter ranges use the following values: Local group galaxies show up with positive as well as negative radial velocities in the range of $-500 \leq v_{\mathrm{LSR}}\,[\mathrm{km\,s^{-1}}] \leq 500$. *hi_21_cm_mag* should be brighter than say 15 mag and *h1_21_cm_50pc_width* ranges between some tens to hundred $\mathrm{km\,s^{-1}}$. The Stockert beam is about 35 arcmin in diameter.

Setting meaningfully the parameters allows you to select galaxies for your observation.

4.10 Observing a pulsar

As discussed in Sec. 2.3 the ionized gas component leads to the dispersion of a pulsar's signal. The most recent catalog of pulsars you can find online ATNF Pulsar Catalogue. A pretty high number of parameters can be set individually to select the appropriate pulsar. Let us consider the most important of them: *DecJ*, *S1400* and *DM*, corresponding to the pulsar's declination and thus its height over the observatory's horizon, the pulsar's flux at 1.4 GHz and the dispersion measure. To guess some constraining values, *S1400* ranges between 20 and 250 Jy, while the dispersion measure is between 20 and 160 $\mathrm{cm^{-3}} \cdot \mathrm{pc}$. Again, you as observers have to find a compromise between distance and the pulsar flux at 21-cm. Large distances yield a high pulsar dispersions but faint fluxes.

By switching between HI 21-cm line and pulsar observations it is necessary to re-configure the backend to the pulsar mode. This will be done manually by the telescope's operator. The next step is to fold the pulsar's signal using the program `sigproc` at the observatories site. This is necessary to extract a high signal–to–noise pulse profile. The folding sums up all individual pulses on the same time frame. For that aim one needs to know the pulse periode. Finally the pulses match exactly in time and can be summed up. `sicproc` splits up the pulse into eight frequency bands. You might consider the largest separation in frequency to calculate the temporal shift between the arrival times.

First step is to calculate the center frequency of each of the eight frequency bands. Next, you determine the channel separation between two frequencies. Note that the pulsar's periode is equally distributed across 256 spectral channels. This means pulse period divided by 256 channels is equal the time resolution (time/channel) of your instrumental setup.

This number for the time resolution you need to multiply with the separation in channels and yields the time gap between both frequencies in units of seconds.

To calculate the dispersion, you need rearrange Eq. 2.4 and to equate for the dispersion measure. Dividing this value by the average electron density of $n_e = 0.03\,\mathrm{cm^{-3}}$ yields the

distance to the pulsar in units of parsec.

CHAPTER 5

Observations

5.1 Data reduction of the HI 21-cm line observations

The HI 21-cm line data will be provided in CSV/ASCII format. You can read it with a standard spread sheet program or by python. The different column are separated by a blank.

Note, that there is a standard header comprising the essential information on your line observation at the very beginning of the file (see Fig. 5.1). Perhaps it is a good idea to separate header and table before importing the table in a spread sheet program.

Essential header information for our purposes are the rest frequency, the channel number of this rest frequency, the integration time and the frequency resolution. These information you need to calculate the distance to the galaxy as well as to calculate the system noise and system temperature.

```
CRVAL3  =              60.54854 / DEC of target
GLAT    =  -0.9999886832499796 / Galactic latitude of target
GLON    =    132.0000090425928 / Galactic longitude of target
EPOCH   =               2000.0 / EPOCH
FRONTEN = '21 cm    '           / Front End
BACKEND = 'AFFTS    '           / Fast Fourier Spektrometer
CALFACT =           0.00068687 / Calibration factor used
CALSOUR = 'UNCALIBRATED'       / Calibration source used
CALTIME = 'NO DATE '           / Calibration date and time
LOFREQ  =         1230000000.0 / Local oscillator frequency
(nominal)          |
LSR-COR =    13.43003376603246 / LSR correction applied in km/sec
LOLSR   =     1229936368.98894 / Local oscillator frequency (LSR
corrected)
FSMODE  =                    F / Frequency switiching mode
DELTAF2 =                  0.0 / Offset for frequency switching
mode
LINE    = 'Hydrogen'           / Line name
BUNIT   = 'K        '          / Units are Kelvin if calibrated
RESTFREQ=         1420405752.0 / Rest frequency
OBSTIME =            19.796616 / Duration of observation
CTYPE1  = 'FREQ     '          / Type of x
CRVAL1  =                    0 / Frequency offset
CDELT1  =         -6103.515625 / Frequency resolution per channel
CRPIX1  =                  389 / Number of reference channel
AZIMUTH =    198.1327099609375 / Azimuth of telescope at start of
observation
ELEVATIO=    79.23183349609374 / Elevation of telescope at start
of observation
DAT-STOP= '2020-03-19'         / Stop date of observation
```

Figure 5.1: Displayed is the header of the Stocker HI 21-cm line profile. This header comprises the essential information about you observation, like time, date, azimuth and elevation. To calculate the system temperature you need the integration time and the frequency resolution. Both are highlightes in yellow.

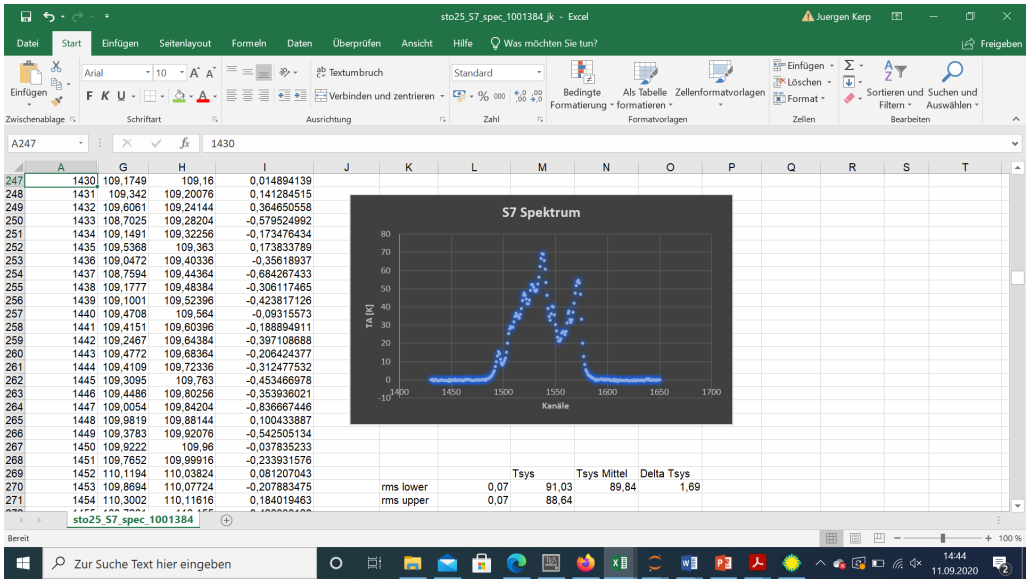

	A	G	H	I
247	1430	109,1749	109,16	0,014894139
248	1431	109,342	109,20076	0,141284515
249	1432	109,6061	109,24144	0,364650558
250	1433	108,7025	109,28204	-0,579524992
251	1434	109,1491	109,32256	-0,173476434
252	1435	109,5368	109,363	0,173833789
253	1436	109,0472	109,40336	-0,35618937
254	1437	108,7594	109,44364	-0,684267433
255	1438	109,1777	109,48384	-0,306117465
256	1439	109,1001	109,52396	-0,423817126
257	1440	109,4708	109,564	-0,09315573
258	1441	109,4151	109,60396	-0,188894911
259	1442	109,2467	109,64384	-0,397108888
260	1443	109,4772	109,68364	-0,206424377
261	1444	109,4109	109,72336	-0,312477532
262	1445	109,3095	109,763	-0,453466978
263	1446	109,4486	109,80256	-0,353936021
264	1447	109,0054	109,84204	-0,836667446
265	1448	109,9819	109,88144	0,100433887
266	1449	109,3783	109,92076	-0,542505134
267	1450	109,9222	109,96	-0,037835233
268	1451	109,7652	109,99916	-0,233931576
269	1452	110,1194	110,03824	0,081207043
270	1453	109,8694	110,07724	-0,207883475
271	1454	110,3002	110,11616	0,184019463

Figure 5.2: Read in the csv/ascii table in a standard spreat sheet program. Use as separators the "space character" or "blank". You will find several columns. Displayed here is the first column, the channel number and the seventh column the antenna temperature T_{A}. For the baseline fit you need only these.

Figure 5.2 displays a scientific valuable HI spectrum obtained with the Stockert telescope. You can identify that the channel number is in column A and T_A in column G. The baseline removes the radio continuum emission from the observed T_A spectrum. As you can deduce from the numbers, the values are pretty high, in excess of 100 K.

You need to remove this radio continuum emission accurately. For this aim "hide" those rows at the bandbass edges as well as the HI 21-cm line emission of your source. Displaying this baseline region shows a linear of little bit more complicated linear structure. Ideally the channels selected for the baseline approximation are located in the immediate neighbourhood of the HI line emission of your source of interest. Use only as many spectral channels as necessary to determine accurately the baseline by a linear approximation. If necessary you might apply a polynomical fit of second or third order. Reducing the number of spectral channels minimizes the baseline order. Note that I shows up, in the baseline region only, with values less than 1 K.

Plotting column A vs. column I yields the baseline subtracted T_A spectrum, as displayed. According to the Kalberla et al. paper you might evaluate the integral across the S7 profile or the peak brightness temperature of the S7 spectrum to determine the calibration factor.

After quantifying the calibration factor you can evalute the system noise at T_B scale. For this aim you calculate the variance of column I across your baseline region. Inserting frequency resolution, integration time and the ΔT_B value for the system noise in the radiometer equation, you know the actual system temperature.

You apply the same procedure to your galaxy of interst. Removing the baseline, determining the calibrated rms of the data and eventually the integral across the galaxy's line profile.

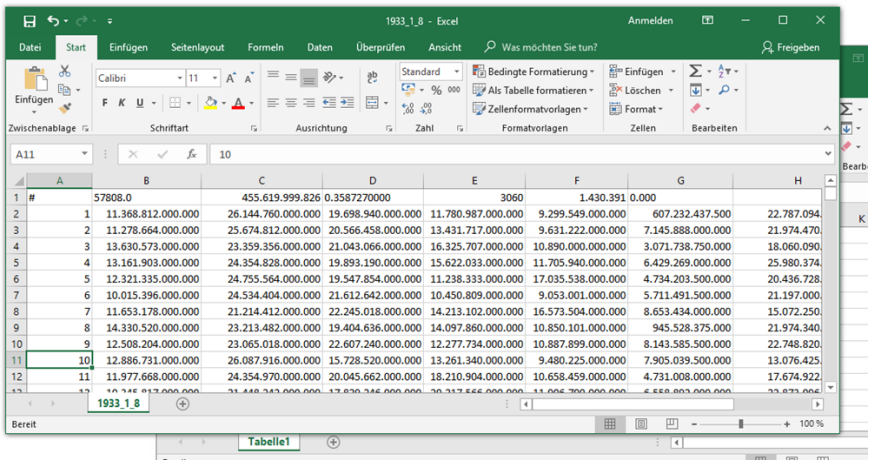

	A	B	C	D	E	F	G	H
1	#	57808.0	455.619.999.826	0.3587270000	3060	1.430.391	0.000	
2	1	11.368.812.000.000	26.144.760.000.000	19.698.940.000.000	11.780.987.000.000	9.299.549.000.000	607.232.437.500	22.787.094.
3	2	11.278.664.000.000	25.674.812.000.000	20.566.458.000.000	13.431.717.000.000	9.631.222.000.000	7.145.888.000.000	21.974.470.
4	3	13.630.573.000.000	23.359.356.000.000	21.043.066.000.000	16.325.707.000.000	10.890.000.000.000	3.071.738.750.000	18.060.090.
5	4	13.161.903.000.000	24.354.828.000.000	19.893.190.000.000	15.622.033.000.000	11.705.940.000.000	6.429.269.000.000	25.980.374.
6	5	12.321.335.000.000	24.755.564.000.000	19.547.854.000.000	11.238.333.000.000	17.035.538.000.000	4.734.203.500.000	20.436.728.
7	6	10.015.396.000.000	24.534.404.000.000	21.612.642.000.000	10.450.809.000.000	9.053.001.000.000	5.711.491.500.000	21.197.000.
8	7	11.653.178.000.000	21.214.412.000.000	22.245.018.000.000	14.213.102.000.000	16.573.504.000.000	8.653.434.000.000	15.072.250.
9	8	14.330.520.000.000	23.213.482.000.000	19.404.636.000.000	14.097.860.000.000	10.850.101.000.000	945.528.375.000	21.974.340.
10	9	12.508.204.000.000	23.065.018.000.000	22.607.240.000.000	12.277.734.000.000	10.887.899.000.000	8.143.585.500.000	22.748.820.
11	10	12.886.731.000.000	26.087.916.000.000	15.728.520.000.000	13.261.340.000.000	9.480.225.000.000	7.905.039.500.000	13.076.425.
12	11	11.977.668.000.000	24.354.970.000.000	20.045.662.000.000	18.210.904.000.000	10.658.459.000.000	4.731.008.000.000	17.674.922.

Figure 5.3: Read in the ascii table in a table calculation program. Use as separators the "space character". The first row contains some header elements only the entry in column "D" is important, it is the pulsar rotation period in units of seconds. Left column is the number of channels (256 in total), the next columns give the intensities in the eight frequency bands.

5.2 Data reduction of a pulsar signal

Your data is stored in an ASCII format. You can read it with any program. Here, we will use a table calculation program.

First read in the ASCII file. Use as seperator the "space character". You will finally have a table with nine columns. The first one is the number of channels running from 1 to 256. In the first row of column "D" you will find the rotation period of your pulsar of interest, here 0.358 seconds. Each channel corresponds to $0.358/256 = 1.4 \cdot 10^{-3}$ seconds.

The columns are

- Column A: time stamp (256 stamps, evenly distributed across the pulsar's rotation periode)
- Column B to I: intensity within the eight subsequent frequency bands

Next we need to calculate the central frequency of the frequency bands. The whole bandpass transmits 98.4 MHz. We divided it into eight bands, each of 12.3 MHz with. The upper frequency limit of the total band is 1430.391 MHz. So the first center frequency is $1430.391 - \frac{12.3\,MHz}{2} = 1424.241$ MHz. The next lower center frequency is 12.3 MHz lower etc.

Plot the channels versus the frequency band intensity allows you to identify the signal. By inspection the different frequency bands you will see the dispersion of the pulse. By evaluating the peak position of the different frequency bands, you evaluate the separation of the pulsar's signal in channels and finally in seconds. Using the Eq. 2.3 you evaluate the dispersion measure and vi Eq. 2.4 estimate the distance to the pulsar.

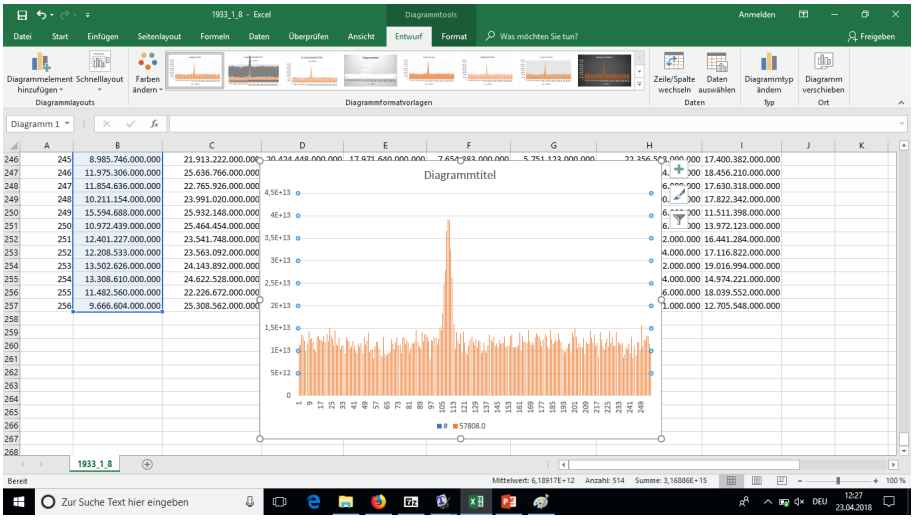

Figure 5.4: Using in the example a simple block diagram, we plot the number of channels versus the intensity of the first data column. The pulsar signal is visible. Determine the pear position in channels for each frequency band allows you to follow the dispersion.

CHAPTER 6

Additional resources

S264, Radio astronomical observing course: advanced laboratory course (physics601)

Revision: January 2022
Note: Double counting experiment

6.1 Aim of the experiment

The radio astronomical course is aiming to provide an early observing experience as well as a practical approach to the technical design of a classical single dish radio telescope. Focusing in particular on the telescope and receiver construction, source selection, data acquisition and reduction. Until today all operating high frequency radio telescopes are constructed in the same way as the 25-m Stockert telescope you are using. We start with the preparation of the experiment by searching online catalogs for suitable radio sources for the day of the observation. At the site we inspect the telescope's primary reflector, identify the location of the antenna feed horn, trace the connections from the feed horn to the amplifier and band-pass. In a subsequent step, we set up the spectrometer and observe a Milky Way standard calibration source. These data will be evaluated to determine the basic parameters of the instrumental setup. A, nearby galaxy is going to be observed and its major physical properties, like gas and total mass and recession velocity will be evaluated. Finally we observe and quantify the dispersion of a pulsar signal to determine its distance.

6.2 Required Knowledge

A basic knowledge on radio astronomy is required. Explicitly you should prepare the following topics:

- right ascension and declination, sideral time, geographic coordinates of the observatory, source visibilty
- basic construction principles of radio telescopes, antenna diagram, angular resolution, surface accuracy
- antenna feed construction, heterodyne principle, construction of a radiometer and its sensitivity, system temperature
- HI 21-cm line, Doppler velocity, local standard-of-rest frame, spectral and temporal resolution, physics of neutron stars and pulsars

- electromagnetic radiation, coherence, dispersion, basics of radition transfer

6.3 Literature

- Lab course script
- Lecture Notes: *Radio Astronomy: Tools, Applications & Impacts* (U.Klein)

Both scripts are available from the tutor and can be either send per mail or be lend as a copy.

6.4 Task description

In the following you will find a brief description of the individual tasks you are going to perform. For details we refer to lab course script.

First part: Source selection

- Select, by applying meaningful constains, an external galaxy and a pulsar from online data bases.
- Determine the geographic location of the Stockert observatory. Qantify the visibility of your sources of interest for the Stockert observatory at the date and time of your observing slot. For this you need the right ascension and declination of the sources of interest.
- Choose at least two or three sources for each type and create a priority list. Radio frequency interferences might affect the observations in a particular direction.

Second part: Exploration of the telescope design

- inspect and identify the basic telescope construction. Explain the advantages and disadvantages of the chosen construction. Discuss and evaluate the telescope primary mirror surface accuracy.
- identify the location of the primary and secondary focus, the location of the antenna feed horn and consequences for the observations to be performed.
- trace the connection between the antenna feed and the amplifier and its relevance for the quality of the receiver's performance. Identify the position of the band-pass, discuss the limitation of this construction.
- discuss the technical design of the receiver and the limitations of the construction in your report.

Third part: Observe a Milky Way standard calibration source. and determine the instrumental sensitivity

- discuss the Rayleigh-Jeans approximation of Planck's law and the relevance for the observation you are performing.
- describe the difference between the antenna temperature T_A and the brightness temperature T_B.
- Choose S7, S8 or B8 as calibration source. Determine the visibility of this source during your observing session.
- Setup the spectrometer and perform the observation. Choose a suitable integration time aiming to quantify signal with a 5% accuracy.
- Evaluate the system temperature and the systematic uncertainties introduced by the chosen approach? You will need later on the derived calibation factor to quantify the HI mass of the external galaxy.

Fourth part: observing a nearby galaxy

- choose a nearby galaxy from the observatory's catalog close to culmination.
- calculate the necessary integration time to determine the galaxy's integrated flux with an accuracy of 10%.
- perform the observation and evaluate the total flux, the peak brightness temperature, the systemic velocity. Discuss the line profile and compare it to that of the calibration source. What are the differences, what are the similarities?
- evaluate the HI mass of the galaxy. Explain the difference to the galaxy's total mass and estimate the total mass. Discuss the limitation of the applied method and ways to improve the results in your report.

Fifth part: determine the distance of a pulsar

- choose an observable pulsar from the observatory's catalog.
- estimate the necessary observing time to detect the pulsar's signal
- perform the observation and use the Pulsar de-disperser to evaluate the arrival times of the pulsar's signal subdivided into eight sub-bands. (Note: you have to perform this task at the telescope's site).
- evaluate the temporal separation between the arrival times of the low and high-frequency pulsar signal. Adopt an electron volume density and estimate the distance between the Earth and the pulsar. Describe step-by-step the performed data reduction process in your report.

6.5 Procedure and analysis

The observed data will be saved in CSV files and will be accessible via `sciebo` shortly after the online session. Download these files to your computer. Details on the data analysis procedure can be found in the course manuscript. All that is needed to perform the data analyses is a standard spreadsheet program or python. According to the actual Sars-Cov-19 measures the observing course is conducted in person according to the regulations by the Bonn University.

Best wishes for a successful experiment!